Available online at www.sciencedirect.com
SCIENCE DIRECT®
Physica D 197 (2004) 242–268
PHYSICA D
www.elsevier.com/locate/physd

The Keplerian regime of charged particles in planetary magnetospheres

Manuel Iñarrea[a], Víctor Lanchares[b], Jesús F. Palacián[c,*], Ana I. Pascual[b], J. Pablo Salas[a,c], Patricia Yanguas[c]

[a] *Área de Física Aplicada, Universidad de la Rioja, 26006 Logroño, Spain*
[b] *Departamento de Matemáticas y Computación, Universidad de la Rioja, 26004 Logroño, Spain*
[c] *Departamento de Matemática e Informática, Universidad Pública de Navarra, Campus de Arrosadía, 31006 Pamplona, Spain*

Received 17 December 2003; received in revised form 24 June 2004; accepted 15 July 2004

Communicated by C.K.R.T. Jones

Abstract

The dynamics of a charged particle orbiting around a rotating magnetic planet is studied. The system is modelled by the two-body Hamiltonian perturbed by an axially-symmetric function which goes to infinity as soon as the particle approaches the planet. The perturbation consists in a magnetic dipole field and a corotational electric field. When it is weak compared to the Keplerian part of the Hamiltonian, we average the system with respect to the mean anomaly up to first order in terms of a small parameter defined by the ratio between the magnetic and the Keplerian interactions. After dropping higher-order terms, we use invariant theory to reduce the averaged system by virtue of its continuous and discrete symmetries, determining also the successive reduced phase spaces. Then, we study the flow of the resulting system in the most reduced phase space, describing all equilibria and their stability, as well as the different classes of bifurcations. Finally, we connect the analysis of the flow on these reduced phase spaces with the one of the original system.

PACS: 02.30.Oz; 05.45.−a; 82.40.Bj; 96.35.−j

Keywords: Planetary magnetospheres; Størmer problem; Perturbed Kepler problems; Averaging the mean anomaly; Equilibria; Stability and bifurcations; Reconstruction of the flow; Periodic orbits and invariant tori

1. Introduction

The theoretical study of the motion of a charged particle in planetary magnetospheres has attracted the attention of physicists and astronomers since the second middle of the last century. The pioneering model goes back to

* Corresponding author. Tel.: +34 948 169554; fax: +34 948 169521.
E-mail address: palacian@unavarra.es (J.F. Palacián).

0167-2780/$ – see front matter © 2004 Published by Elsevier B.V.
doi:10.1016/j.physd.2004.07.009

Størmer's work in 1907 (see the papers [38] and the monography [39]), where the motion of a charge in a pure magnetic dipole field (the *Størmer model*) is considered. This model provides satisfactory results for the explanation of the dynamics of light particles (ions or electrons) which are present in the radiation belts surrounding magnetized planets [11,12]. However, when charged dust grains are considered, the ratio between the charge and the mass of the particle is small and the purely magnetic model has to be improved. The reason is that one takes into account the gravitational field created by the planet, as well as the corotational electric field due to the rotation of the planet (see [20] and references therein). This is the so-called *generalised Størmer* model, which will be denoted from now on by the acronym *GS*.

In a recent series of very interesting papers, the *GS* model has been revisited by Horányi, Howard and coworkers [22,24,23,13]. The authors use a *GS* model that includes Keplerian gravity, a magnetic dipole aligned along the axis of rotation of the planet and a corotational electric field. In this framework, due to the axial symmetry of the system, the third component of the angular momentum is an integral, and the dynamics of the charged dust grain is governed by a two-dimensional effective potential. This potential has been intensively explored. Specifically, the above-mentioned authors achieve the following: (i) the global stability conditions of the grain are obtained as a function of the parameters [24]; and (ii) the existence of non-equatorial halo orbits [23,13] for the grain is predicted.

Our aim is to describe the global dynamics of the *GS* problem. It is a nice candidate to which apply the modern analytic tools of nonlinear dynamics. However, the dynamics is highly nonlinear and it is extremely difficult to state a global analytic model that explains the complete motion of the grain. Roughly speaking, in the *GS* problem the grain is subjected to gravitational and electromagnetic forces, which are in competition. The result of this fight depends on the charge–mass ratio of the grain. So, the dynamics of the grain can be either gravitationally or electromagnetically dominated [24].

If the dynamics of the grain is electromagnetically dominated, the Keplerian term in the effective potential can be taken as a perturbation of the electromagnetic terms. The effective potential is very complex, and among other things, it presents non-equatorial potential wells where halo orbits survive [24,23]. On the other hand, if the Keplerian gravity dominates, we can argue the existence of a perturbed Keplerian potential well where the grain is trapped. This is the situation we deal with in this paper.

The study is mainly performed from an analytical point of view. We consider the Hamiltonian representing the *GS* problem as a sum of a pure Keplerian part and a perturbation describing the magnetic dipole field and the corotational electric field. The basic idea is to transform our original system into an equivalent one, which is defined through an integrable Hamiltonian function and is, therefore, easier to be studied. Moreover, the simplified system contains the main features of the original one. Thus, we can extract dynamical information of the original system from the integrable Hamiltonian.

We achieve the transformation to the new dynamical system in three steps. First, by assuming that the electromagnetic term is weak compared to the Keplerian one, we apply the Delaunay normalisation [10] up to first order. From this transformation, we obtain the averaged (or *normalised*) Hamiltonian with a new formal integral L (the *Keplerian symmetry*) representing the positive square root of the semi-major axis of the perturbed Keplerian ellipses, and where only two degrees of freedom remain in the Hamiltonian. Secondly, the axial symmetry of the problem allows one to reduce to one the degrees of freedom of the system. This symmetry is also used to obtain the two-dimensional phase space (the so-called *twice-reduced phase space*) related to the new system. Third, we exploit the finite symmetries of the original Hamiltonian in order to simplify the appearance of the differential equations and the shape of the two-dimensional phase space as much as possible. This last step is achieved through a new reduction mapping which gives rise to the so-called fully-reduced Hamilton function defined in a new phase space, called the *fully-reduced phase space*.

After this process is concluded, the reduced system is of one degree of freedom, hence integrable. Then, we analyse, as a function of the parameters, the dynamical features of this system, calculating its equilibria and bifurcations. An estimation of the error committed in the normalisation procedure allows us to conclude that our approach is valid in a neighbourhood of the origin (e.g. the Keplerian regime). This is reinforced using some Poincaré surfaces of section. Moreover, using reconstruction of the flow techniques, we infer that the bifurcations of the relative

equilibria correspond to bifurcations of two-dimensional invariant tori and quasi-periodic orbits of the original Hamiltonian.

Other studies on particles around planetary magnetospheres using the tools of nonlinear analysis were given by Braun [2,3]. In particular, Braun dealt with the Størmer problem and introducing high-order normal forms combined with KAM theory, he was able to find out some two-dimensional invariant tori and quasi-periodic orbits. Our approach is in the same spirit as Braun's work. However, our model is different as we use the *GS* Hamiltonian in the Keplerian regime. Besides, we achieve a global analysis of the system resulting after normalisation and reduction, using for that an appropriate parameterization of the reduced phase space.

As stated by Howard et al [23], it is very important to understand the nonlinear dynamics of the orbital motion of charged particles around magnetic planets. Furthermore, it is indeed a live issue, as it is shown by some projects as the Cassini mission on tour around Saturn to perform detailed *in situ* measurements of charged dust grains, which arrived on July 1, 2004, or the Bepi-Colombo mission to explore Mercury's magnetosphere, supposed to be launched by ESA in 2008 [19].

The paper is structured as follows. The problem is formulated in Section 2. In Section 3, we apply the Delaunay normalisation. In Section 4, the Keplerian, the axial symmetries as well as the finite symmetries allow us to obtain the different reduced phase spaces of the normalised system. The dynamics in the fully-reduced phase space is the subject of Section 5. It involves the determination of equilibria, bifurcations and the analysis of the stability. The phase flow of the reduced system is described in Section 6. In Section 7, we establish the connection between the reduced and the original systems, estimating the error related to the averaging process. Poincaré surfaces of section are provided in order to validate the error estimations and our results. Moreover, some periodic orbits are approximated from the set of quasi-periodic trajectories, using the finite symmetries of the problem. The conclusions appear in Section 8.

2. The problem

In the problem at hand, we assume that a particle of mass m and charge q is orbiting around a rotating magnetic planet of mass M and radius R. The general Hamiltonian of this particle in Gaussian units is then expressed as:

$$\mathcal{H} = \frac{1}{2m}\left(\mathbf{P} - \frac{q}{c}\mathbf{A}\right)^2 + U(\mathbf{x}), \tag{1}$$

where c is the speed of the light in the vacuum, $\mathbf{x} = (x, y, z)$ corresponds to the Cartesian coordinates and $\mathbf{P} = (P_x, P_y, P_z)$ represents the conjugate momenta of $\mathbf{x}$. Besides, $\mathbf{A}$ represents the vector potential describing the magnetic forces and $U(\mathbf{x})$ is the scalar potential accounting for the electric and gravitational interactions. The magnetic field $\mathbf{B}$ of the planet is supposed to be a perfect magnetic dipole of strength μ aligned along the north–south poles of the planet (the z-axis). Thus, if $r = \sqrt{x^2 + y^2 + z^2}$ stands for the distance of the charged particle to the centre of mass of the planet, the vectors $\mathbf{A}$ and $\mathbf{B}$ are:

$$\mathbf{A} = \frac{\mu}{r^3}(-y, x, 0), \qquad \mathbf{B} = \nabla \times \mathbf{A}. \tag{2}$$

If we assume that the planet's magnetosphere is a rigid conducting plasma which rotates with the same angular velocity $\Omega = (0, 0, \omega)$ as the planet, the charge q is subjected to a corotational electric field $\mathbf{E}$ of the form:

$$\mathbf{E} = -\frac{1}{c}(\Omega \times \mathbf{x}) \times \mathbf{B} = -\frac{\mu\omega}{c}\nabla\Psi, \quad \text{where} \quad \Psi = \frac{x^2 + y^2}{r^3}. \tag{3}$$

The combined Keplerian and electrostatic forces give the potential:

$$U(\mathbf{x}) = -\frac{Mm}{r} + \frac{q\mu\omega}{c}\Psi. \tag{4}$$

By introducing the expressions (2) and (4) into (1), we get the Hamiltonian:

$$\mathcal{H} = \frac{1}{2m}(P_x^2 + P_y^2 + P_z^2) - \frac{Mm}{r} - \frac{\mu q}{mc}\frac{H}{r^3} + \frac{\mu^2 q^2}{2mc^2}\frac{x^2+y^2}{r^6} + \frac{q\mu\omega}{c}\Psi, \tag{5}$$

where $H = xP_y - yP_x$ is the z-component of the angular momentum.

Since the above Hamiltonian is invariant under rotations around the z-axis, H is an integral and cylindrical variables $(\rho, z, \phi, P_\rho, P_z, H)$ arise in a natural way. Hence, in these variables (5) reads:

$$\mathcal{H} = \frac{1}{2m}\left(P_\rho^2 + P_z^2 + \frac{H^2}{\rho^2}\right) - \frac{Mm}{r} - \omega_c R^3\frac{H}{r^3} + \frac{m\omega_c^2 R^6}{2}\frac{\rho^2}{r^6} + \frac{m\omega\omega_c R^3}{c}\frac{\rho^2}{r^3}. \tag{6}$$

The parameter $\omega_c = (qB_0)/(mc)$ stands for the *cyclotron* frequency, where $B_0 = \mu/R^3$ designates the magnetic field strength at the planetary equator.

In order to analyse the dynamics, it is convenient to use dimensionless coordinates and momenta. Firstly, we define the new coordinates as functions of the planet radius R, e.g. $\mathbf{x}' = \mathbf{x}/R$, $\mathbf{P}' = \mathbf{P}/(mR\omega_K)$. As well we define a new (dimensionless) time $t' = \omega_K t$, where $\omega_K = \sqrt{M/R^3}$ is the *Keplerian frequency*. After introducing the above-mentioned transformations in (6) and dropping primes in coordinates and momenta, we arrive at the following dimensionless Hamiltonian:

$$\mathcal{H}' = \frac{\mathcal{H}}{mR^2\omega_K^2} = \frac{1}{2}\left(P_\rho^2 + P_z^2 + \frac{H^2}{\rho^2}\right) - \frac{1}{r} - \delta\frac{H}{r^3} + \delta\beta\frac{\rho^2}{r^3} + \frac{\delta^2}{2}\frac{\rho^2}{r^6}. \tag{7}$$

To avoid tedious notation, from now on we also drop the prime of the previous Hamiltonian. In (7), we have defined the parameters $\delta = \omega_c/\omega_K$ and $\beta = \omega/\omega_K$, which indicate, respectively, the ratio between the magnetic and the Keplerian interactions and the ratio between the electrostatic and Keplerian interactions. For a given planet B_0, ω and ω_K are constant and hence the problem depends on three parameters. On the one hand, on the internal parameters H and $\mathcal{H} = E$ (the energy), and on the other hand, on the external parameter δ which indicates the charge–mass ratio q/m of the particle.

As stated in Section 1, the goal of this paper is to study the dynamics of the system when the main effect on the particle is assumed to be the Keplerian gravity. In other words, we are interested in those cases where the motion takes place inside of a Keplerian potential well. Moreover, this potential well must be located outside the planetary region in order to consider realistic orbits. In this way, we introduce the effective potential U_{eff} from (7) as:

$$U_{\text{eff}} = \frac{H^2}{2\rho^2} - \frac{1}{r} - \delta\frac{H}{r^3} + \delta\beta\frac{\rho^2}{r^3} + \frac{\delta^2}{2}\frac{\rho^2}{r^6}.$$

In the pure Keplerian case ($\delta = 0$), the function U_{eff} has a minimum at $z = 0$ and $\rho = H^2$ (for $H \neq 0$). The points r_+ and r_-, where the particle's velocity is zero (the turning points), tend monotonically to $H^2/2$ and $+\infty$, respectively, as U_{eff} tends to 0. In this way, only values of $|H| > \sqrt{2}$ guarantee that r_- and r_+ are outside the planet. For a planet like Saturn, the spin rate is $\omega \approx 1.64 \times 10^{-4}$ rad/s, and the parameter $\beta \approx 0.4$ (see Murray and Dermott [33]). Hence, if $|\delta| \ll 1$ and $\beta < 1$, we can assume that the Keplerian potential well is only slightly affected by the terms depending on the electromagnetic interactions. This fact can be observed in Fig. 1a, from which we infer that a deformed Keplerian well exists for $|\delta| \leq 0.01$. Other values of δ and β should be used if we considered the magnetospheres of other giant planets. From now on we shall consider δ and β as parameters, so that our analysis could be used for other planets although we shall allow that δ varies in $[-0.01, 0.01]$ whereas β will be between 0 and 0.5, which includes Saturn's value. For more details on the ranges of β and δ, see [33,18].

The critical points (ρ_0, z_0) of U_{eff} are the solutions of the system of equations: $(\partial U_{\text{eff}}/\partial\rho, \partial U_{\text{eff}}/\partial z) = (0, 0)$. In order to analyse how the presence of the perturbations distorts the Keplerian well, we study analytically the evolution of the roots located at the ρ-axis. For $z = 0$, $\partial U_{\text{eff}}/\partial z = 0$, and the first equation (for $H \neq 0$) gives the

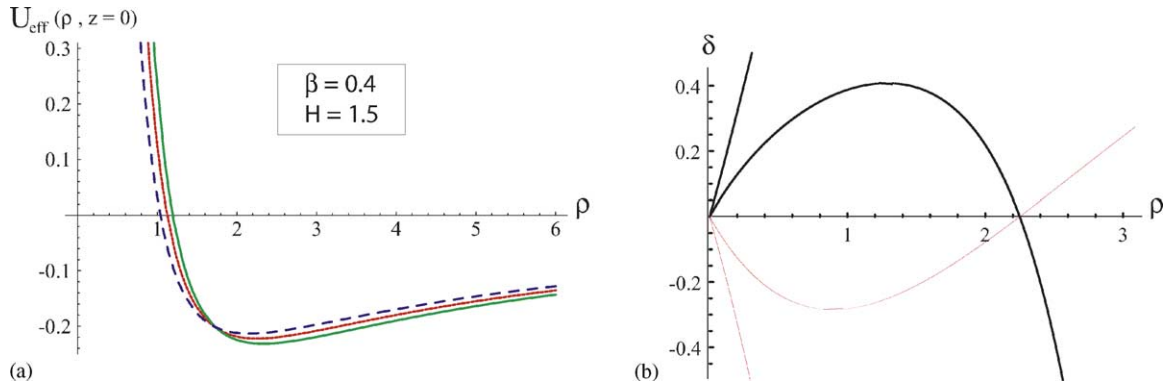

Fig. 1. (a) Effective potential U_{eff} defined in the plane $z = 0$ for $\delta = 0$ (solid line), for $\delta = 0.01$ (dashed line) and $\delta = -0.01$ (pointed line). In all curves, the values for H and β are $H = 1.5$ and $\beta = 0.4$. (b) Evolution of the critical points (ρ_0, z_0) of the effective potential U_{eff} in the interval $\delta \in [-0.5, 0.5]$ for $\beta = 0.4$, $H = -1.5$ (red line) and $H = 1.5$ (black line). (For interpretation of the references to colour in this figure legend, the reader is referred to the web version of the article.)

following third-degree polynomial equation:

$$\mathcal{P}(\rho) = -2\delta^2 + 3\delta H\rho - H^2\rho^2 + \rho^3 - \beta\delta\rho^3 = 0.$$

For $H = \pm 1.5$ and $\beta = 0.4$, the evolution of the roots of $\mathcal{P}$ as a function of δ is shown in Fig. 1b. For $H = -1.5$, we observe that $\mathcal{P}$ has only one root for $\delta > 0$, while for $\delta < 0$ it has either one or three roots. For $H = 1.5$, we find the same qualitative behaviour, but for opposite sign of δ. In both situations, the smallest root corresponds to an inner minimum, whereas the middle one to a saddle point and the biggest one to the Keplerian minimum. The disappearance of the Keplerian well occurs when the saddle and the Keplerian minimum tend one to the other giving rise to a double root and disappearing thereafter. Only the inner minimum remains. Note that if $\delta \in [-0.1, 0.1]$, the Keplerian well is far enough from the saddle. This is why the well is only slightly deformed by the electromagnetic perturbations.

3. Delaunay normalisation

3.1. Canonical variables

Hamiltonian (7) can be seen as a perturbed Kepler problem. There are certain sets of variables well suited to deal with this type of systems. As we will make an extensive use of them, we describe briefly their main features.

Polar-nodal variables: $(r, \vartheta, \nu, P_r, \Theta, N)$ were introduced by Jacobi, but used explicitly later by Whittaker [41]. The action Θ designates the modulus of the angular momentum vector $\mathbf{G} = \mathbf{x} \times \mathbf{P}$ in the synodic frame. The angle conjugate to Θ is the argument of the latitude $0 \leq \vartheta < 2\pi$ through the radial direction. Besides, r, has already been introduced and its conjugate momentum P_{r} denotes the radial velocity in the synodic frame. The angle of the node, ν, is the variable conjugate to N. In the region of the phase space where $\mathbf{G}$ does not vanish, we decompose it uniquely as $\mathbf{G} = \Theta\mathbf{n}$ with $\Theta > 0$ and $\|\mathbf{n}\| = 1$. The vector $\mathbf{n}$ indicates the normal direction and is orthogonal to the plane spanned by $\mathbf{x}$ and $\mathbf{P}$: the *instantaneous orbital plane*. Its inclination with respect to the equatorial plane is given by the angle $I \in (0, \pi)$ with $N = \Theta \cos I$ and N is the third component of $\mathbf{G}$ in the synodic frame. Some types of trajectories cannot be studied with these variables. They are not useful for collision ($r \equiv 0$), rectilinear ($\Theta \equiv 0$) or equatorial orbits ($\Theta \equiv |N|$).

Delaunay variables: (ℓ, g, h, L, G, H) are a set of action-angle variables defined through polar-nodal variables by means of a generating function built with the "mixed" set of variables $(r, \vartheta, \nu, L, G, H)$. We do not detail the construction of these variables, but we address the reader to references [9,10] for that.

If $\mathcal{H}_0$ stands for the Hamiltonian of the two-body problem, the action L is related to the two-body energy by the identity $\mathcal{H}_0 = -1/(2\,L^2)$. The action G is the modulus of the angular momentum, thus $G \equiv \Theta$. The third component of $\mathbf{G}$ is H, i.e. $H \equiv N$. The angle ℓ is named the mean anomaly. The eccentricity of the orbit is designated by e, which in terms of Delaunay actions reads $e = \sqrt{1 - G^2/L^2}$; as $e \in (0, 1)$ then $G \in (0, L)$. Circular orbits are not accessible in Delaunay variables in order to ensure that ℓ would be well defined. The true anomaly f is expressed as: $r(1 + e\,\cos\,f) = G^2$. The semi-major axis a of the ellipse is related with L by the identity $L^2 = a$. The angle g is the argument of the pericentre. It is reckoned from the ascending node of the orbit in the instantaneous orbital plane, then $g = \vartheta - f$. The angle h is the argument of the node, i.e. $h \equiv \nu$. Relations among all quantities can be looked up in [4].

Delaunay variables are not valid for circular, collision, rectilinear and equatorial orbits. Polar-nodal and Delaunay variables will be used to normalise the two-degree-of-freedom Hamiltonian (7) and reduce it to another one of one degree of freedom. This will be accomplished in Section 4.

Hamiltonian (7) in "mixed" Delaunay and polar-nodal variables reads as:

$$\mathcal{H} = -\frac{1}{2L^2} - \frac{\delta H}{r^3} + \frac{\delta(\delta + 2\beta r^3)}{4r^4}[1 + \cos^2\,I + \sin^2\,I\,\cos(2\vartheta)], \tag{8}$$

where $\cos\,I$ refers to the quotient H/G.

Now, in order to apply a perturbation theory, we split $\mathcal{H}$ into two pieces. As $-1/(2L^2)$ is the leading term of $\mathcal{H}$ we identify it with the unperturbed part of the Hamiltonian, that is, with $\mathcal{H}_0$. Hence, the rest of $\mathcal{H}$ is placed at first order, so we make $\mathcal{H}_1 = \mathcal{H} + 1/(2L^2)$. Thus, our system can be considered a perturbation of the two-body problem since we have $|\mathcal{H}_1| \ll |\mathcal{H}_0|$. We could have put the terms factored by δ^2 at second order and perform a second-order theory. However, we have preferred to achieve a first-order theory as the formulae are not so cumbersome.

3.2. Normalisation through first-order averaging

The goal of this subsection is to transform Hamilton function (8) into another Hamiltonian $\mathcal{K} = \mathcal{K}_0 + \mathcal{K}_1$, such that $\mathcal{K}_0 \equiv \mathcal{H}_0$ via a formal symplectic change of coordinates $\Phi : (\ell, g, h, L, G, H) \longrightarrow (\ell', g', h', L', G', H')$ and a generating function $\mathcal{W} = \mathcal{W}_1$. Up to first order the transformation is given by:

$$\begin{aligned} &\ell' = \ell + \frac{\partial \mathcal{W}_1}{\partial L}, \qquad g' = g + \frac{\partial \mathcal{W}_1}{\partial G}, \qquad h' = h + \frac{\partial \mathcal{W}_1}{\partial H}, \\ &L' = L - \frac{\partial \mathcal{W}_1}{\partial \ell}, \qquad G' = G - \frac{\partial \mathcal{W}_1}{\partial g}, \qquad H' = H - \frac{\partial \mathcal{W}_1}{\partial h}, \end{aligned} \tag{9}$$

where $\mathcal{W}_1$ is written in terms of the old variables (without primes). This is indeed the so-called inverse change of variables truncated at order one.

The direct change $\alpha : (\ell', g', h', L', G', H') \longrightarrow (\ell, g, h, L, G, H)$ puts the old variables as functions of the new ones through $\mathcal{W}_1$ written in terms of the new variables. We remark that Φ is the inverse change of α and vice versa. If we push the computation to a certain order M, after truncation of higher-order terms, the new Hamiltonian will be independent of the mean anomaly and subsequently, $\mathcal{K}$ will enjoy the action L as a new integral. The process to perform this transformation is called *Delaunay normalisation* (see [9,10]); the steps to get the averaged (normalised) Hamiltonian are summarized next.

Let $n = 1/L^3$ be the mean motion of the infinitesimal body orbiting the planet, thus the physical dimensions of n are [1/time]. So, the Lie operator associated with $\mathcal{H}_0$ is $n\,\partial(\cdot)/\partial\ell$. Our interest is to perform a first-order theory calculating $\mathcal{K}_1$ and $\mathcal{W}_1$. The reason for not pushing the calculations to higher orders is that the first-order

Hamiltonian retains all qualitative information we need, as all the equilibrium points we shall get out of the analysis of the reduced equations will be isolated, in order words, the first-order reduced system will be structurally stable (see [31]). This will be seen in full detail in Section 5.

From now on we drop the primes of the variables so as to avoid tedious notation. At first order, the transformed Hamiltonian is going to be $\mathcal{K} = \mathcal{K}_0 + \mathcal{K}_1$, where $\mathcal{K}_1$ must be independent of ℓ. Thus, $\mathcal{K}$ will define a system of two degrees of freedom in g, h, G and H. We will have that the Poisson bracket $\{\mathcal{K}_i,\ \mathcal{H}_0\} = 0$ for $i = 0, 1$.

The Delaunay normalisation is carried out straightforwardly and in closed form for the eccentricity and for the mean anomaly, although some difficulties arise when doing the computations. This is circumvented using some adequate changes of variables defined through the eccentric and the true anomalies [34,35].

We identify $\mathcal{H}_0 \equiv \mathcal{K}_0$ and solve the homology equation:

$$n\frac{\partial \mathcal{W}_1}{\partial \ell} + \mathcal{K}_1 = \mathcal{H}_1,$$

by taking

$$\mathcal{K}_1 = (2\pi)^{-1}\int_0^{2\pi} \mathcal{H}_1\,\mathrm{d}\ell \quad \text{and} \quad \mathcal{W}_1 = n^{-1}\int (\mathcal{H}_1 - \mathcal{K}_1)\,\mathrm{d}\ell.$$

Thus, we arrive at the Hamiltonian:

$$\begin{aligned}
&\mathcal{K} = \mathcal{K}_0 + \mathcal{K}_1, \quad \text{with} \quad \mathcal{K}_0 = -\frac{1}{2L^2},\\
&\mathcal{K}_1 = \frac{\delta}{16L^5G^7(L+G)}[2(L+G)(4\beta L^3G^7 + 4\beta L^3G^5H^2 - \delta G^4 - 8L^2G^4H - \delta G^2H^2\\
&\qquad + 3\delta L^2G^2 + 3\delta L^2H^2) + (L-G)(G^2-H^2)(8\beta L^3G^5 + \delta G^2 + 2\delta LG + \delta L^2)\cos(2g)],
\end{aligned} \tag{10}$$

together with its generating function defined up to first order, $\mathcal{W} = \mathcal{W}_1$:

$$\begin{aligned}
\mathcal{W}_1 = \frac{\delta}{48L^2G^7(L^2-G^2)r^2}&\{6(L^2-G^2)r^3(-8L^2G^4H\varphi r - \delta G^4\varphi r - \delta G^2H^2\varphi r + 3\delta L^2G^2\varphi r\\
&+ 3\delta L^2H^2\varphi r + \delta L^2G^5P_r + \delta L^2G^3H^2P_r - 8L^2G^5HrP_r + 3\delta L^2G^3rP_r + 3\delta L^2GH^2rP_r\\
&+ 4\beta L^2G^7r^2P_r + 4\beta L^2G^5H^2r^2P_r) + (G^2-H^2)r(-48\beta L^4G^6\varphi r^3 + 3\delta G^4\varphi r^3 - 6\delta L^2G^2\varphi r^3\\
&+ 3\delta L^4\varphi r^3 + 6\delta L^4G^7P_r - 2\delta L^4G^5rP_r - 3\delta L^2G^5r^2P_r + \delta L^4G^3r^2P_r + 48\beta L^4G^7r^3P_r\\
&- 5\delta L^2G^3r^3P_r + 3\delta L^4Gr^3P_r + 24\beta L^2G^7r^4P_r + 24\beta L^4G^5r^4P_r)\cos(2g) + 2L^4G^6(G^2-H^2)\\
&\times[3\delta G^2 - 4\delta r + 24\beta G^2r^3 - 24\beta r^4\,\log(G^2/r)]\sin(2g)\},
\end{aligned}$$

where $\varphi = f - \ell$. In our computations, we have not used techniques based on Fourier expansions in the mean, eccentric or true anomaly, neither Taylor expansions in the eccentricity. So, as we are working with compact expressions we can analyse any type of elliptic motion, and we do not care if a trajectory is highly eccentric. Moreover, polylogarithmic functions would be introduced in the generating functions of the corresponding orders bigger than one due to the appearance of φ and $\log(G^2/r)$ at first order, see for example [34].

The construction of $\mathcal{K}_i$ and $\mathcal{W}_i$ for $i \geq 1$ is required to compute the expressions of the invariant manifolds related to the original Hamiltonian vector field with high accuracy. Besides, if we stop at order one, the explicit formula of $\mathcal{W}_1$ is used to build the direct and inverse change of coordinates, which is essential to estimate the error committed after truncating the averaged Hamiltonian. Moreover, it is also required that the error committed after truncation

be maintained controlled in a certain domain of the Delaunay variables, see also [36] and the example therein. We shall come back to this in Section 7, when reconstructing the flow of the original Hamiltonian system.

Note that $\mathcal{K}$ and $\mathcal{W}$ are well defined whether $0 < G < L$ and $r > 0$. So rectilinear, circular and collision orbits should be excluded from the study. However, circular trajectories will be considered as a limit situation of our approach using appropriate variables.

4. Reductions and reduced phase spaces

4.1. Passage to $S^2_L \times S^2_L$

The next step of our approach consists in expressing $\mathcal{K}$ in terms of the appropriate invariants associated with the symmetries of the problem.

The integrals associated with $\mathcal{K}$ are the functions which are constant on the solutions of the system defined by $\mathcal{H}_0$. All these integrals can be expressed as functions of L, the components of the angular momentum vector $\mathbf{G} = (G_1, G_2, G_3)$ (we remark that $G_3 \equiv H$) and the Laplace vector $\mathbf{A}_\mathrm{L} = (A_1, A_2, A_3)$, i.e. the vector defined as $\mathbf{A}_\mathrm{L} = \mathbf{P} \times \mathbf{G} - \mathbf{x}/\|\mathbf{x}\|$. Note that $\|\mathbf{G}\| = G$, $\|\mathbf{A}_\mathrm{L}\| = e$ and $\mathbf{G} \cdot \mathbf{A}_\mathrm{L} = 0$. We consider the mapping:

$$\varphi_L : \mathbf{R}^6 \setminus (\{\mathbf{0}\} \times \mathbf{R}^3) \longrightarrow \mathbf{R}^6 : (\mathbf{x}, \mathbf{P}) \mapsto (\mathbf{a}, \mathbf{b}) \equiv (\mathbf{G} + L\mathbf{A}_\mathrm{L}, \mathbf{G} - L\mathbf{A}_\mathrm{L}),$$

with $\mathbf{a} = (a_1, a_2, a_3)$ and $\mathbf{b} = (b_1, b_2, b_3)$. Explicitly, the functions a_i and b_i can be given in terms of Delaunay variables [6]. Henceforth, the quantities G, H, $\cos\, g$, $\sin\, g$, $\cos\, h$, $\sin\, h$, $\cos\, I$ and $\sin\, I$ can be easily expressed in terms of $\mathbf{a}$ and $\mathbf{b}$ and the positive constant L. Now, a Hamiltonian independent of ℓ can be written as a function of the invariants $\mathbf{a}$ and $\mathbf{b}$ and the constant $L > 0$.

Now, fixing a value of $L > 0$, the product of the two-sphere:

$$S^2_L \times S^2_L = \{(\mathbf{a}, \mathbf{b}) \in \mathbf{R}^6 \mid a_1^2 + a_2^2 + a_3^2 = L^2, \quad b_1^2 + b_2^2 + b_3^2 = L^2\} \tag{11}$$

is the phase space associated with Hamiltonian systems of Keplerian type independent of ℓ, that is, perturbed Keplerian Hamiltonians for which L is an integral. This result was first reported by Moser [32] using a regularisation technique based on stereographic projections. Later, it has been described and used by Cushman [6]. Note that $S^2_L \times S^2_L$ is a four-dimensional smooth space and therefore the reduction is regular [30]. The introduction of the invariants extends the use of Delaunay and polar-nodal variables, as equatorial, circular and rectilinear orbits are included [6,35].

4.2. Reduction of the axial symmetry

Now we briefly analyse what happens for systems invariant under the axial symmetry, that is, for Hamiltonians independent of h. We start by fixing a value of H (with $|H| \leq G$), this integral H can be understood as an S^1-action, or the action of the one-dimensional unitary group $U(1)$ over the space of coordinates and momenta such that:

$$\varrho : S^1 \times (\mathbf{R}^6 \setminus (\{\mathbf{0}\} \times \mathbf{R}^3)) \longrightarrow \mathbf{R}^3 \times \mathbf{R}^3 : \quad (R_z(h), (\mathbf{x}, \mathbf{P})) \mapsto (R_z(h)\mathbf{x}, R_z(h)\mathbf{P}), \tag{12}$$

where $R_z(h)$ is the matrix of a rotation by an angle h about the z-axis, with $0 \leq h < 2\pi$. This is a singular action because there are non-trivial isotropy groups. Indeed, $\{(0, 0, z) \mid z \in \mathbf{R}\}$ is invariant under all rotations around the z-axis. Thus, the reduction due to the axial symmetry is singular, in contrast to the regular reduction obtained by doing L an integral, where all the isotropy groups were trivial. Then, we have to apply a singular reduction treatment [1].

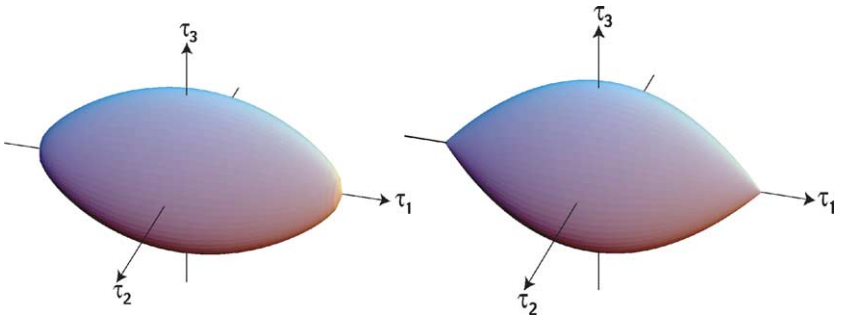

Fig. 2. Twice-reduced phase spaces $\mathcal{T}_{L,H}$ and $\mathcal{T}_{L,0}$. On the left $L = 10$ and $H = 2$, in this case $\mathcal{T}_{10,2}$ is diffeomorphic to a two-sphere. On the right, we have taken $L = 11$ and $H = 0$, hence $\mathcal{T}_{11,0}$ corresponds to a two-sphere with two singular points.

If we denote $\tau = (\tau_1, \tau_2, \tau_3)$, we can define the mapping:

$$\pi_H : S_L^2 \times S_L^2 \longrightarrow \{H\} \times \mathbf{R}^3 : (\mathbf{a}, \mathbf{b}) \mapsto (H, \tau_1, \tau_2, \tau_3) \equiv (H, \tau), \quad \text{with}$$
$$\tau_1 = \tfrac{1}{2}(a_3 - b_3), \quad \tau_2 = a_1 b_2 - a_2 b_1, \quad \tau_3 = a_1 b_1 + a_2 b_2. \tag{13}$$

The corresponding phase space is defined as:

$$\mathcal{T}_{L,H} = \pi_H(S_L^2 \times S_L^2) = \{\tau \in \mathbf{R}^3 \mid \tau_2^2 + \tau_3^2 = [(L + \tau_1)^2 - H^2][(L - \tau_1)^2 - H^2]\}, \tag{14}$$

for $0 \le |H| \le L$ and $L > 0$. Note that τ_2 and τ_3 always belong to the interval $[H^2 - L^2, L^2 - H^2]$, whereas τ_1 belongs to $[|H| - L, L - |H|]$. The two-dimensional phase spaces $\mathcal{T}_{L,H}$ and $\mathcal{T}_{L,0}$ (the phase space for $H = 0$) are plotted in Fig. 2 for fixed values of the parameters L and H.

In [6], it is proven that whether $0 < |H| < L$, $\mathcal{T}_{L,H}$ is diffeomorphic to a two-sphere S^2 and therefore the reduction is regular in that region of the phase space. However, when $H = 0$, $\mathcal{T}_{L,0}$ is a topological two-sphere with two singular points: the vertices at $(\pm L, 0, 0)$. The reason for the existence of these two points is that the S^1-action ϱ has two fixed points: $L\,(\pm 1, 0, 0, \mp 1, 0, 0)$ and consequently it is not free. Finally, when $|H| = L$ the phase space $\mathcal{T}_{\pm L,L}$ gets reduced to a point. See also two applications on the reduction of perturbed Keplerian systems in [8,37].

Rectilinear motions satisfy $G = H = 0$. Taking also into account the constraint (14), we conclude that they are defined on the one-dimensional set $\mathcal{R}e_{L,0} = \{\tau \in \mathbf{R}^3 \mid \tau_2 = 0, \tau_3 = \tau_1^2 - L^2\}$. Thus, excepting orbits with $\|\mathbf{x}\| = 0$ we could analyse rectilinear trajectories. Circular type of orbits are located on a unique point of $\mathcal{T}_{L,H}$ with coordinates $(0, 0, L^2 - H^2)$—or on a unique point of $\mathcal{T}_{L,0}$ with coordinates $(0, 0, L^2)$—whereas equatorial trajectories are represented in the negative extreme point of $\mathcal{T}_{L,H}$ with coordinates $(0, 0, H^2 - L^2)$ (respectively, at the point $(0, 0, -L^2)$ of $\mathcal{T}_{L,0}$).

It is not difficult to prove that Delaunay variables not involving the angles ℓ and h can be expressed in terms of τ [6,35]. So, the twice-reduced system is represented by a Hamiltonian expressed in terms of τ. If we define $\tau_4 = \sqrt{L^2 + H^2 - \tau_1^2 + \tau_3}$, after dropping constant terms, Hamiltonian (10) is written as the rational function:

$$\bar{\mathcal{K}} = \frac{\delta}{4L^5\tau_4^7[4L\tau_4 + \sqrt{2}(2L^2 + \tau_4^2)]}\{\delta(2L^2 + 2\sqrt{2}L\tau_4 + \tau_4^2)[\tau_4^2(14L^2 - 4\tau_1^2 - 3\tau_4^2) + H^2(20L^2 - 2\tau_4^2)]$$
$$+ 8L^2\tau_4^4[-2H(2L^2 + 2\sqrt{2}L\tau_4 + \tau_4^2) + \beta L\tau_4^2(2H^2L + \sqrt{2}(L^2 + H^2 - \tau_1^2)\tau_4 + L\tau_4^2)]\}. \tag{15}$$

4.3. Reduction of the finite symmetries

In the next paragraphs, we follow similar steps to those of Cushman and coworkers [8,15] in their treatment of the Zeeman–Stark effect.

First, we notice that the original Hamilton function $\mathcal{H}$ enjoys the following discrete symmetries:

$$\begin{aligned}
&\mathcal{R}_1 : (x, y, z, P_x, P_y, P_z) \longrightarrow (x, -y, -z, -P_x, P_y, P_z),\\
&\mathcal{R}_2 : (x, y, z, P_x, P_y, P_z) \longrightarrow (x, -y, z, -P_x, P_y, -P_z),\\
&\mathcal{R}_3 : (x, y, z, P_x, P_y, P_z) \longrightarrow (x, y, -z, P_x, P_y, -P_z).
\end{aligned} \tag{16}$$

It is clear that $\mathcal{R}_3$ can be expressed as the combination of $\mathcal{R}_1$ and $\mathcal{R}_2$. These $\mathbf{Z}_2$-symmetries are conserved through the two previous reductions. Besides, in terms of the τ's, the finite symmetries (reflections) read as follows:

$$\begin{aligned}
&\mathcal{R}_1 : (\tau_1, \tau_2, \tau_3) \longrightarrow (-\tau_1, \tau_2, \tau_3),\\
&\mathcal{R}_2 : (\tau_1, \tau_2, \tau_3) \longrightarrow (\tau_1, -\tau_2, \tau_3),\\
&\mathcal{R}_3 : (\tau_1, \tau_2, \tau_3) \longrightarrow (-\tau_1, -\tau_2, \tau_3).
\end{aligned}$$

Now $\bar{\mathcal{K}} \equiv \bar{\mathcal{K}}(\tau_1^2, -, \tau_3; \delta, \beta, L, H)$ and therefore it enjoys the symmetries $\mathcal{R}_1$, $\mathcal{R}_2$ and $\mathcal{R}_3$, as it should be expected. Hence, it is possible to further reduce Hamiltonian $\bar{\mathcal{K}}$. In this way, we introduce new functions with the aim of taking advantage of these discrete symmetries. Indeed, we define:

$$\sigma_1 = (L - |H|)^2 - \tau_1^2, \qquad \sigma_2 = \frac{\sqrt{L^2 + H^2 - \tau_1^2 + \tau_3}}{\sqrt{2}}. \tag{17}$$

We have chosen a different set of invariants from those selected by Cushman and coworkers [8,15], as we have preferred to use the Delaunay variable G as one of the invariants ($\sigma_2 = G$), so that we can interpret the results of Sections 5–7 in an easier manner.

The inverse change of Eq. (17) is given by:

$$\tau_1 = \pm\sqrt{L^2 + H^2 - 2L|H| - \sigma_1}, \qquad \tau_3 = -\sigma_1 + 2\sigma_2^2 - 2L|H|. \tag{18}$$

The reduction process is now achieved by using a suitable map. We define:

$$\sigma_{L,H} : \mathcal{T}_{L,H} \longrightarrow \mathcal{U}_{L,H} : (\tau_1, \tau_2, \tau_3) \mapsto (\sigma_1, \sigma_2) \quad \text{for} \quad 0 \le |H| \le L,$$

such that σ_1 and σ_2 are given through (17). The resulting space is the most reduced phase space, that is, the fully-reduced phase space and is denoted by $\mathcal{U}_{L,H}$ and, for $H = 0$, by $\mathcal{U}_{L,0}$.

The fully-reduced phase spaces for $H \neq 0$ and $H = 0$ (see Fig. 3) are given, respectively, by:

$$\begin{aligned}
&\mathcal{U}_{L,H} = \{(\sigma_1, \sigma_2) \in \mathbf{R}^2 \mid \frac{(\sigma_2^2 - L|H|)^2}{\sigma_2^2} \le \sigma_1 \le (L - |H|)^2, |H| \le \sigma_2 \le L\},\\
&\mathcal{U}_{L,0} = \{(\sigma_1, \sigma_2) \in \mathbf{R}^2 \mid \sigma_2^2 \le \sigma_1 \le L^2, \quad 0 \le \sigma_2 \le L\}.
\end{aligned} \tag{19}$$

The constraints between the new invariants are deduced from (14) and define the boundaries of $\mathcal{U}_{L,H}$ and $\mathcal{U}_{L,0}$:

$$\begin{aligned}
&\text{if } |H| > 0: \quad \sigma_1\sigma_2^2 = (\sigma_2^2 - L|H|)^2 \quad \text{and} \quad \sigma_1 = (L - |H|)^2,\\
&\text{if } H = 0: \quad \sigma_1 = \sigma_2^2, \quad \sigma_2 = 0 \quad \text{and} \quad \sigma_1 = L^2.
\end{aligned}$$

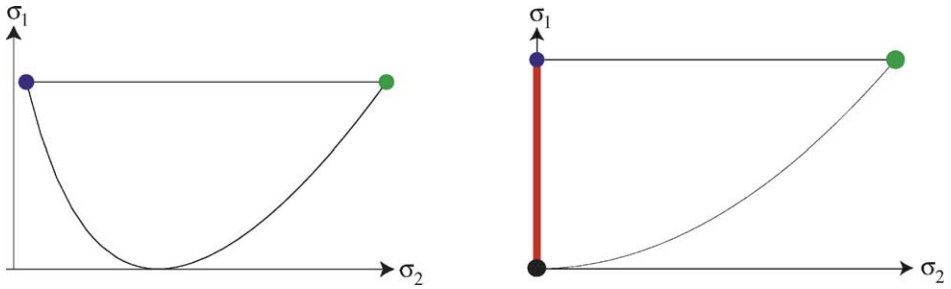

Fig. 3. On the left, fully-reduced phase space for $|H| > 0$. The coordinates of the extreme points of $\mathcal{U}_{L,H}$ are $((L-|H|)^2, |H|)$ (equatorial motions: blue) and $((L-|H|)^2, L)$ (circular motions: green), whereas the space reaches its lowest point at $(0, \sqrt{L|H|})$. On the right, fully-reduced phase space for $H = 0$. The coordinates of the extreme points of $\mathcal{U}_{L,0}$ are $(L^2, 0)$ (polar equatorial motions: blue), (L^2, L) (polar circular motions: green) and $(0, 0)$ (the non-spurious singular point of $\mathcal{U}_{L,0}$: black). The red segment corresponds to rectilinear motions. (For interpretation of the references to colour in this figure legend, the reader is referred to the web version of the article.)

Note that σ_1 and σ_2, together with the constraints inherited from τ, are used to define the spaces $\mathcal{U}_{L,H}$ and $\mathcal{U}_{L,0}$ from the reduction of the twice-reduced phase spaces $\mathcal{T}_{L,H}$ and $\mathcal{T}_{L,0}$. First we note that the spaces $\mathcal{U}_{L,H}$ and $\mathcal{U}_{L,0}$ are, as $\mathcal{T}_{L,H}$ and $\mathcal{T}_{L,0}$, two-dimensional since the reduction comes from discrete symmetries. However, we only need two generators to define $\mathcal{U}_{L,H}$ and $\mathcal{U}_{L,0}$ instead of the three generators used to obtain $\mathcal{T}_{L,H}$ and $\mathcal{T}_{L,0}$.

The space $\mathcal{U}_{L,H}$ has two singular points: $((L-|H|)^2, |H|)$ and $((L-|H|)^2, L)$ while $\mathcal{U}_{L,0}$ has three singular points: $(L^2, 0)$, (L^2, L) and $(0, 0)$. The singularities of $\mathcal{U}_{L,H}$ have been introduced through the mapping $\sigma_{L,H}$ and are indeed spurious. As well the singularities $(L^2, 0)$, (L^2, L) have been introduced by reducing out the discrete symmetries and they are spurious too. The point $(0, 0)$ is the singularity coming from the singular points $(\pm L, 0, 0)$ of $\mathcal{T}_{L,0}$.

We remark that σ_1 and σ_2 are indeed invariants under the action of the three finite symmetries $\mathcal{R}_1$, $\mathcal{R}_2$ and $\mathcal{R}_3$. Moreover, σ_1 is a function that depends on the modulus of the angular momentum and on the argument of pericentre, whereas σ_2 is exactly the modulus of the angular momentum vector. We have:

$$G = \sigma_2, \quad \cos g = \pm\sqrt{\frac{L^2H^2 - 4\sigma_1\sigma_2^2 + 4\sigma_2^4 - 2L|H|(\sigma_1 + 2\sigma_2^2)}{5L^2H^2 - 4(L^2+H^2)\sigma_2^2 + 4\sigma_2^4 - 2L|H|(L^2+H^2-2\sigma_2^2)}},$$
$$\sin g = \pm\sqrt{\frac{4L^2H^2 - 4(L^2+H^2-\sigma_1)\sigma_2^2 - 2L|H|(L^2+H^2-\sigma_1-4\sigma_2^2)}{5L^2H^2 - 4(L^2+H^2)\sigma_2^2 + 4\sigma_2^4 - 2L|H|(L^2+H^2-2\sigma_2^2)}}. \tag{20}$$

From Eq. (18) and the constraint (14), it is readily deduced that a single point in the interior of $\mathcal{U}_{L,0}$ or $\mathcal{U}_{L,H}$ is in correspondence with four points in the space $\mathcal{T}_{L,0}$ or in $\mathcal{T}_{L,H}$, respectively. Besides, a single point in the regular part of the boundaries of either $\mathcal{U}_{L,0}$ or $\mathcal{U}_{L,H}$ is, respectively, related to two points of $\mathcal{T}_{L,0}$ or of $\mathcal{T}_{L,H}$. In addition to this, to each of the two singular points of the boundary of $\mathcal{U}_{L,H}$, it corresponds one point of $\mathcal{T}_{L,H}$. Finally, the points of $\mathcal{U}_{L,0}$ with coordinates $(L^2, 0)$ and (L^2, L) are related, respectively, to the points $(0, 0, -L^2)$ and $(0, 0, L^2)$ on $\mathcal{T}_{L,0}$ whereas the point whose coordinate is $(0, 0)$ in $\mathcal{U}_{L,0}$ corresponds to the singular points $(\pm L, 0, 0)$ of $\mathcal{T}_{L,0}$. This remark will be taken into consideration in Section 5 for discussing the number of critical points of the reduced Hamiltonian under study and in Section 7 for reconstructing the flow of the original system.

We remark that equatorial, rectilinear and circular type of motions are easily characterised in the fully-reduced phase space. For locating circular "trajectories" we need that $\sigma_2 = L$, and so the set of circular "orbits" is zero-dimensional and is defined by the point $((L-|H|)^2, L)$ in $\mathcal{U}_{L,H}$ and by (L^2, L) in $\mathcal{U}_{L,0}$. For equatorial "orbits" we make $\sigma_2 = |H|$, henceforth the set of equatorial "orbits" is defined by the points $((L-|H|)^2, |H|)$ in $\mathcal{U}_{L,H}$ and by $(L^2, 0)$ in $\mathcal{U}_{L,0}$. Finally, rectilinear "orbits" define a one-dimensional set in $\mathcal{U}_{L,0}$ that, since $\sigma_2 = 0$, is simply characterised by the segment of $\mathcal{U}_{L,0}$ given by $(\sigma_1, 0)$ with $(0 \le \sigma_1 \le L^2)$. This type of special motions is depicted in Fig. 3.

4.4. The fully-reduced Hamilton function

From (17), we easily deduce that $\tau_1^2 = (L - |H|)^2 - \sigma_1$ and $\tau_4 = \sqrt{2}\sigma_2$. Hence, Hamiltonian $\bar{\mathcal{K}}$ can be expressed in terms of the new invariants σ_1 and σ_2 as:

$$\bar{\bar{\mathcal{K}}} = \frac{\delta}{16L^5\sigma_2^7(L+\sigma_2)^2}\{\delta(L+\sigma_2)^2[5L^2H^2 - (3H^2 - 4L|H| - 5L^2 - 2\sigma_1)\sigma_2^2 - 3\sigma_2^4] + 16L^2\sigma_2^4[-L^2H - 2LH\sigma_2 + H(-1+\beta L^2H)\sigma_2^2 + \beta L(2L|H| + \sigma_1)\sigma_2^3 + \beta L^2\sigma_2^4]\}. \tag{21}$$

Notice that $\bar{\bar{\mathcal{K}}}$ is singular for $\sigma_2 = 0$. It is not a surprise as σ_2 is equivalent to G and the original Hamilton function $\mathcal{H}$ is not well defined for rectilinear trajectories. A way to circumvent this trouble is based on regularisation techniques, but this is outside the purpose of the present paper. Nevertheless we need to be very careful when analysing orbits with σ_2 small, since the perturbation $\bar{\bar{\mathcal{K}}}$ could be bigger than the unperturbed part and therefore our study could have no sense for almost rectilinear trajectories. In Sections 5 and 7, we shall show how to avoid this problem by controlling the size of $|\bar{\bar{\mathcal{K}}}|$.

5. Relative equilibria and bifurcations

5.1. Equilibrium points and bifurcation diagram

To analyse the equilibria of the system, we neglect those terms in δ^2 in (21). Their influence modifies nor the description of bifurcations neither the stability character of the equilibria of the Hamiltonian:

$$\mathcal{Z} = \frac{\beta L\sigma_2^2[\sigma_1\sigma_2 + L(|H| + \sigma_2)^2] - H(L+\sigma_2)^2}{L^3\sigma_2^3(L+\sigma_2)^2}, \tag{22}$$

obtained from $\bar{\bar{\mathcal{K}}}$ after dropping the common factor δ. This is because we do not take into account those points corresponding to collision "orbits", which are not relevant from a physical point of view.

Equilibria are now determined by the extremum points of (22) on the reduced space $\mathcal{U}_{L,H}$. Taking into account that $\partial\mathcal{Z}/\partial\sigma_1 = \beta/[L^2(L+\sigma_2)^2]$ does not vanish for any value of σ_2, there is no equilibrium points in the interior of $\mathcal{U}_{L,H}$ and, consequently, they are located on the boundary.

Note that there always exist two equilibrium points, those points where the two curves delimiting the boundary of $\mathcal{U}_{L,H}$ meet. These are the points:

$$E_1 \equiv ((L-|H|)^2, |H|), \qquad E_2 \equiv ((L-|H|)^2, L),$$

corresponding to the class of equatorial and circular "orbits", respectively.

To determine the rest of the equilibria, if any, two cases must be considered:

(a) those equilibria located on the rectilinear part of the boundary given by the curve $\sigma_1 = (L-|H|)^2$, under the restriction $|H| \le \sigma_2 \le L$;
(b) those equilibria located on the curved part of the boundary defined by $\sigma_1\sigma_2^2 = (\sigma_2^2 - L|H|)^2$ and $|H| \le \sigma_2 \le L$.

5.1.1. Case (a)

If $\sigma_1 = (L - |H|)^2$, then (22) turns into the single real-valued function:

$$\mathcal{Z}(\sigma_2) = \frac{\beta L\sigma_2^2(L\sigma_2 + H^2) - H(L + \sigma_2)}{L^3\sigma_2^3(L + \sigma_2)}. \tag{23}$$

The extremum values are reached at $\sigma_2 = |H|$, $\sigma_2 = L$ (discussed previously) and at those points satisfying:

$$\frac{\mathrm{d}\mathcal{Z}(\sigma_2)}{\mathrm{d}\sigma_2} = \frac{3H(L + \sigma_2)^2 - \beta L\sigma_2^2(L\sigma_2^2 + 2H^2\sigma_2 + LH^2)}{L^3\sigma_2^4(L + \sigma_2)^2} = 0.$$

In this case, σ_2 must be a root in the interval $(|H|, L)$ of the polynomial:

$$\mathcal{P}(\sigma_2) = 3H(L + \sigma_2)^2 - \beta L\sigma_2^2(L\sigma_2^2 + 2H^2\sigma_2 + LH^2).$$

As $\mathcal{P}(\sigma_2)$ is a fourth-degree polynomial it is possible to derive explicitly the coordinates of the equilibria. However, it is not easy to decide whether they are real or complex or they belong to the interval $(|H|, L)$. For this reason, we focus on the number of roots rather than on their explicit expressions.

By means of the Descartes rule of signs, we can decide on the number of positive real roots by counting the number of sign changes in the coefficient sequence of polynomial $\mathcal{P}$. For retrograde motions ($H < 0$) all coefficients are positive and $\mathcal{P}$ has no positive real roots. In this case there are no equilibria.

On the other hand, for prograde "orbits" ($H \geq 0$) the coefficients of the third and fourth powers of σ_2 are positive, whereas the independent term as well as the first power of σ_2 are negative. Thus, no matter the sign of the second power is, the total number of sign changes is one, and $\mathcal{P}$ has a unique real positive root. Bolzano's theorem ensures that the root is located in the interval $(|H|, L)$ if and only if $\mathcal{P}(|H|)\mathcal{P}(L) < 0$, i.e. when the following condition is fulfilled:

$$(3\beta L^2H^2 + \beta L^4 - 12H)[2\beta LH^3 - 3(L + H)] < 0. \tag{24}$$

If σ_2^* is the root of $\mathcal{P}$ satisfying (24), we have the equilibrium:

$$E_3 \equiv ((L - |H|)^2, \sigma_2^*).$$

Note that E_3 appears or disappears whenever one crosses the hypersurfaces:

$$\Gamma_1 \equiv 3\beta L^2H^2 + \beta L^4 - 12H = 0, \qquad \Gamma_2 \equiv 2\beta LH^3 - 3(L + H) = 0. \tag{25}$$

5.1.2. Case (b)

If $\sigma_1\sigma_2^2 = (\sigma_2^2 - L|H|)^2$, (22) turns into the single real-valued function:

$$\mathcal{Z}(\sigma_2) = \frac{\beta L\sigma_2(\sigma_2^3 + LH^2) - H(L + \sigma_2)}{L^3\sigma_2^3(L + \sigma_2)}. \tag{26}$$

As in the previous case, $\sigma_2 = |H|$ and $\sigma_2 = L$ are extremum values and the rest are obtained from:

$$\frac{\mathrm{d}\mathcal{Z}(\sigma_2)}{\mathrm{d}\sigma_2} = \frac{3H(L + \sigma_2)^2 + \beta L^2\sigma_2(\sigma_2^3 - 2LH^2 - 3H^2\sigma_2)}{L^3\sigma_2^4(L + \sigma_2)^2} = 0.$$

This equation is satisfied if σ_2 is a root of the fourth-degree polynomial:

$$\mathcal{Q}(\sigma_2) = 3H(L+\sigma_2)^2 + \beta L^2\sigma_2(\sigma_2^3 - 3H^2\sigma_2 - 2LH^2).$$

The maximum number of sign changes in its coefficient list is two for $H > 0$. For retrograde orbits ($H < 0$), the number of sign changes is one, provided that all coefficients are negative except that of the fourth power of σ_2.

Descartes rule of signs ensures the existence of a positive root σ_2^- for retrograde motions and, thus, the existence of a possible equilibrium point if σ_2^- is located in the interval $(|H|, L)$. This is the case if $\mathcal{Q}(-H)\mathcal{Q}(L) < 0$. Since

$$\mathcal{Q}(-H) = H(L-H)(2\beta L^2H^2 + 3L - 3H)$$

is sign-defined (negative) for $H \neq 0$, we obtain an equilibrium point if $\mathcal{Q}(L) > 0$, that is, whether the condition

$$5\beta L^2H^2 - \beta L^4 - 12H < 0 \tag{27}$$

is fulfilled. This equilibrium point has coordinates:

$$E_0 \equiv \left(\frac{(\sigma_2^{-2} + LH)^2}{\sigma_2^{-2}}, \sigma_2^-\right)$$

and appears or disappears as it is crossed the hypersurface obtained from (27):

$$\Gamma_0 \equiv 5\beta L^2H^2 - \beta L^4 - 12H = 0. \tag{28}$$

For the case of prograde motions, we need further insight in order to determine the number of roots of $\mathcal{Q}$. We take advantage of the resultant (see [5]) of a polynomial to compute the boundary between none and two positive roots, which corresponds to the appearance of a double root. In this way:

$$\mathrm{Res}\left(\mathcal{Q}, \frac{\mathrm{d}\mathcal{Q}}{\mathrm{d}\sigma_2}\right) = 432\beta^3L^8H^3(L^2-H^2)(3H - 8\beta L^2H^2 + 16\beta L^4 + 6\beta^2L^4H^3 - \beta^4L^8H^5) = 0. \tag{29}$$

Excluding the cases $\beta = 0$, $H = 0$ and $L = 0$, (29) vanishes if $L^2 - H^2 = 0$ or if its last factor vanishes. For $L = |H|$, $\mathcal{Q}$ has a double root at $\sigma_2 = -L$ and then it is when the last factor of $\mathrm{Res}(\mathcal{Q}, \mathrm{d}\mathcal{Q}/\mathrm{d}\sigma_2)$ vanishes when $\mathcal{Q}$ has a positive double root. Furthermore, $\mathcal{Q}$ has two positive real roots if

$$-3H + 8\beta L^2H^2 - 16\beta L^4 - 6\beta^2L^4H^3 + \beta^4L^8H^5 > 0. \tag{30}$$

Moreover, when (30) is satisfied then:

- if $\mathcal{Q}(H) > 0$ and $\mathcal{Q}(L) > 0$, then $\mathcal{Q}$ has two roots in the interval (H, L),
- if $\mathcal{Q}(H) < 0$ and $\mathcal{Q}(L) > 0$, then $\mathcal{Q}$ has a root in the interval (H, L),
- if $\mathcal{Q}(H) < 0$ and $\mathcal{Q}(L) < 0$, then $\mathcal{Q}$ has no roots in the interval (H, L).

We note that it is not possible that $\mathcal{Q}(H) > 0$ and $\mathcal{Q}(L) < 0$ at the same time, so the three items above are exhaustive.

In short, for prograde "orbits" ($H \geq 0$) two equilibria can be obtained:

$$E_4 \equiv \left(\frac{(\sigma_{20}^2 - LH)^2}{\sigma_{20}^2}, \sigma_{20}\right), \qquad E_5 \equiv \left(\frac{(\sigma_{21}^2 - LH)^2}{\sigma_{21}^2}, \sigma_{21}\right),$$

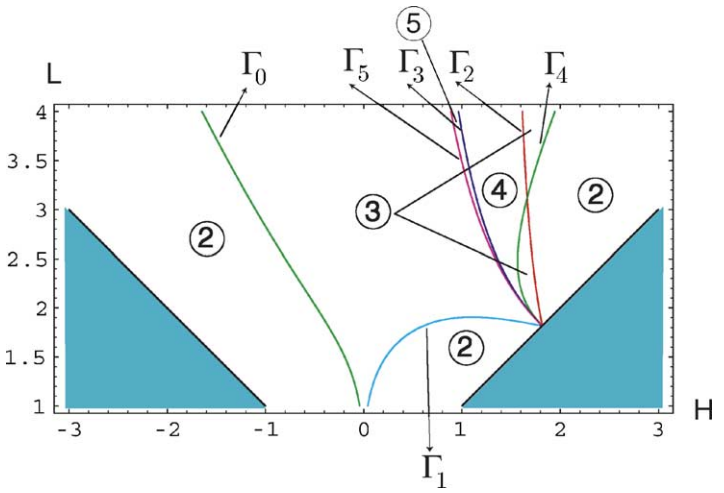

Fig. 4. Plane of parameters (H, L) for $\beta = 0.4$. The number of equilibria in each region delimited by the curves Γ_k appears encircled.

where σ_{20} and σ_{21} are the two positive real roots of $\mathcal{Q}$. Moreover, these points appear or disappear when crossing the hypersurfaces defined through:

$$\Gamma_3 \equiv 2\beta L^2 H^2 - 3(L + H) = 0, \qquad \Gamma_4 \equiv \beta L^2(L^2 - 5H^2) + 12H = 0,$$
$$\Gamma_5 \equiv -3H + 8\beta L^2 H^2 - 16\beta L^4 - 6\beta^2 L^4 H^3 + \beta^4 L^8 H^5 = 0. \tag{31}$$

From the discussion above it follows that, once β is fixed, the plane (H, L) is divided into different regions where the number of equilibria changes. These regions are determined by the curves defined by (25), (28) and (31) together with the constraint $|H| \leq L$ as it is depicted in Fig. 4.

Some remarks of special interest must be noticed. The first one is that Γ_0 and Γ_4 are defined by the same equation, but they appear in Fig. 4 as two branches of the algebraic equation. The second one is that all curves are coincident on the line $L = H$, just on the boundary of the plane of parameters at:

$$P = \left(\sqrt[3]{\frac{3}{\beta}}, \sqrt[3]{\frac{3}{\beta}}\right).$$

The third remark is that all lines Γ_k correspond to parametric bifurcations of pitchfork type except for Γ_5 that corresponds to a saddle-centre bifurcation. This conclusion follows from the number of equilibrium points involved in the bifurcation together with the Index Theorem and a theorem on the multiplicity of a root for a vanishing resultant.

5.2. Stability

The linear stability of the equilibria can be decided through their character as extremum points, not only relatively to the boundary but to the whole fully-reduced phase space. In this sense, a relative maximum or minimum in the boundary does not imply a stable equilibrium. It is necessary that it keeps its character with respect to a neighbourhood containing points in the interior of the fully-reduced phase space. However, Hamiltonian (22) is an increasing function of σ_1 for constant σ_2. This means that, for constant σ_2, the Hamiltonian ranges from a minimum value in the lower bound of the reduced phase space (curved part of the boundary) to a maximum value in the upper

bound (straight part of the boundary). Consequently, a local maximum in the straight part of the boundary is stable whereas an unstable point corresponds to a minimum. The reverse situation is satisfied in the curved part of the boundary, a minimum implies stability, while a maximum implies instability.

In the case of the extremum points of the boundary, i.e. the points E_1 and E_2, their stability can be discussed by means of a similar argument. Considering the Hamiltonian restricted to the straight and curved parts of the boundary, the two functions so defined must be increasing or decreasing at the same time. That is to say, the sign of the derivatives of the two real-valued functions (23) and (26) must be the same. Thus, E_1 is stable if

$$[2\beta L H^3 - 3(L+H)][2\beta L^2 H^2 - 3(L+H)] > 0. \tag{32}$$

Note that the two factors in (32) are the polynomials defining Γ_2 and Γ_3. Then, E_1 is stable except for the region between Γ_2 and Γ_3.

In the same way, E_2 is stable if the condition

$$(3\beta L^2 H^2 + \beta L^4 - 12H)(5\beta L^2 H^2 - \beta L^4 - 12H) > 0 \tag{33}$$

is fulfilled. This is the case outside the region between Γ_0, Γ_1 and Γ_4.

The point E_3 is stable if it is a maximum. A straightforward calculation yields:

$$\left.\frac{\mathrm{d}^2\mathcal{Z}}{\mathrm{d}\sigma_2^2}\right|_{E_3} \equiv -\beta L\sigma_2^{*2}(L^2H^2 + 3LH^2\sigma_2^* + 2L^2\sigma_2^{*2} + H^2\sigma_2^{*2} + L\sigma_2^{*3}) < 0,$$

since $|H| \le \sigma_2^* \le L$. Consequently, E_3 is stable when it exists.

An interesting consequence is the presence of a saddle-connection bifurcation. Note that E_3 appears after a pitchfork bifurcation involving E_1 and it disappears through a pitchfork bifurcation involving E_2. Then, the homoclinic loops attached to equilibria E_1 and E_2 eventually merge and then interchange the stable points they encircle. This happens when the energy for E_1 and E_2 "orbits" is the same, that is, the saddle-connection takes place when:

$$\Gamma_6 \equiv \beta\, L^2\, H^2\, (L+H) - 2\,(L^2 + LH + H^2) = 0.$$

This equation defines the curve Γ_6 in the plane of parameters, which is located in between Γ_3 and Γ_4 and is tangent to them at the point P.

Finally, the stability of the points E_0, E_4 and E_5 in the curved part of the boundary of the phase space follows from the sign of the second derivative of the Hamiltonian. This reduces to check the sign of the polynomial:

$$\chi(\sigma_2) = \sigma_2^4 + 2L\sigma_2^3 - 2LH^2\sigma_2 - L^2H^2 \tag{34}$$

evaluated at the σ_2-coordinate of the equilibrium points: σ_2^-, σ_{20} and σ_{21}. This polynomial has a root in the interval $(|H|, L)$. Let $\bar{\sigma_2}$ be such a root, then if the σ_2-coordinate of an equilibrium satisfies $\sigma_2 < \bar{\sigma_2}$, it is unstable and stable if $\sigma_2 > \bar{\sigma_2}$. In the limit case, $\chi(\sigma_2) = 0$, σ_2 must be a common root of the polynomials $\mathcal{Q}(\sigma_2)$ and $\chi(\sigma_2)$ and then the resultant of the two polynomials vanishes. The resultant reads now as:

$$\mathrm{Res}(\mathcal{Q}, \chi) = -27L^4H^3(L-H)^2(L+H)^2 \times (-3H + 8\beta L^2H^2 - 16\beta L^4 - 6\beta^2L^4H^3 + \beta^4L^8H^5),$$

and it vanishes with $\mathrm{Res}(\mathcal{Q}, d\mathcal{Q}/d\sigma_2)$ at Γ_5. Then, the points E_4 and E_5 conserve their stability properties while they exist. Moreover, the sign of $\chi(\sigma_2)$ is constant for a root σ_2 of $\mathcal{Q}$ unless Γ_5 is reached. Thus, for prograde "orbits" the lowest root, say σ_{20}, corresponds to an unstable equilibrium (eventually it becomes smaller than H). On the other hand, the equilibrium E_5 is stable because the corresponding root σ_{21} becomes bigger than L.

For $H < 0$, the equilibrium E_0 is stable, because its σ_2-coordinate becomes bigger than L. Moreover, this equilibrium only exists for $H < 0$. Thus, $H = 0$ defines another bifurcation line. We can understand that the point

moves passing from the curved part of the boundary of the fully-reduced phase space (the point E_0 for $H < 0$) to the straight part of the boundary (E_3 for $H > 0$).

6. Phase flow evolution

A complementary information about the dynamics of the system (21) is given by the phase flow evolution. Since the twice-reduced Hamiltonian $\bar{\mathcal{K}}$ (or the fully-reduced one $\bar{\bar{\mathcal{K}}}$) defines a dynamical system of one degree of freedom, the trajectories, after fixing a value E of the energy, result as the intersections of the Hamiltonian $\bar{\mathcal{K}}$ with the surface (14), that is to say, they are the level curves of the equation $\bar{\mathcal{K}} = E$ on (14). Similarly, we can obtain the trajectories of the system in the fully-reduced phase spaces $\mathcal{U}_{L,H}$ and $\mathcal{U}_{L,0}$. It allows us to plot the phase flow of the system quite rapidly and very accurately. In fact, we do not draw the level curves, but we assign to every point on the phase space the value that Hamiltonian $\bar{\mathcal{K}}$ or $\bar{\bar{\mathcal{K}}}$ takes at it. Hence, those points associated with the same value belong to the same level curve $\bar{\mathcal{K}} = E$ (or $\bar{\bar{\mathcal{K}}} = E$). This is the basic idea of the technique known as *painting by number* (see [21]).

Calculations involved in the determination of the phase flow are straightforward. First, we construct a two-dimensional grid which is, either orthographically projected on $\mathcal{T}_{L,H}$ or on $\mathcal{T}_{L,0}$, or directly constructed on the fully-reduced phase spaces $\mathcal{U}_{L,H}$ and $\mathcal{U}_{L,0}$. Then, the Hamiltonian is evaluated at the corresponding points according to the grid we have chosen.

Thereafter, the resulting matrix is submitted as an input in the commercial software TRANSFORM [40], which computes and draws the level curves on the selected orthographic projection or planar space. This technique has been used to produce all the pictures appearing within this section.

Based on the bifurcation diagram obtained in the previous section, we study the phase flow evolution choosing a "representative" path on the parametric plane (H, L) for which the stability and the number of equilibria change. This path surrounds the special point P where all the bifurcation lines Γ_i intersect. Most of the bifurcations experimented by the fully-reduced system along this path will be shown only in $\mathcal{T}_{L,H}$, due to the difficulties of visualizing the phase flow on the fully-reduced phase space $\mathcal{U}_{L,H}$. Here, all changes in the number and stability of equilibria occur in a tiny region of the phase space, therefore it is almost impossible to appreciate the flow evolution.

Fig. 5 shows the evolution of the system in both phase spaces $\mathcal{T}_{L,H}$ and $\mathcal{U}_{L,H}$ for $H = 1.5$ and increasing L from 1.75 to 1.9 along a path crossing the bifurcation line Γ_1. For $L = 1.75$, the phase flow on $\mathcal{T}_{1.75,1.5}$ consists only in rotations around the stable equilibria E_1 and E_2. These rotations correspond to straight lines that surround the equilibria E_1 and E_2 in the fully-reduced phase space $\mathcal{U}_{1.75,1.5}$. When the system reaches the curve Γ_1 a pitchfork bifurcation takes place at equilibrium E_2 which becomes unstable. A separatrix passing through E_2 surrounds two new stable equilibria, namely E_3 and $\bar{E}_3$. This pitchfork bifurcation can also be observed in the fully-reduced phase space $\mathcal{U}_{L,1.5}$, where the equilibrium E_2 becomes unstable and a "semi-separatrix", asymptotic to E_2, surrounds a new stable equilibrium E_3 located at the line $\sigma_1 = (L - |H|)^2$. We remark that the two points E_3 and $\bar{E}_3$ correspond to the same equilibrium point E_3 in $\mathcal{U}_{L,H}$ or $\mathcal{U}_{L,0}$. This duplication follows immediately from Eq. (18) and it is consequence of the discrete symmetries of the problem.

Fig. 6 represents the phase flow evolution of the system in $\mathcal{T}_{L,H}$ along a path crossing the bifurcation lines Γ_5, Γ_3 and Γ_6, for $H = 1.5$ and increasing L from 2 to 2.26. When the system reaches the curve Γ_5, a closed orbit around the equilibrium E_1 experiences a double saddle-centre bifurcation in such a way that four new equilibria appear: two of them unstable, E_4 and $\bar{E}_4$, and the other two of stable character, E_5 and $\bar{E}_5$. Besides, a new heteroclinic orbit connecting E_4 and $\bar{E}_4$ surrounds the centres E_1, E_5 and $\bar{E}_5$. As the system gets close to the bifurcation curve Γ_3, the equilibria E_1, E_4 and $\bar{E}_4$ approach one each other in such a way that when Γ_3 is crossed, another pitchfork bifurcation occurs: the equilibria E_1, E_4 and $\bar{E}_4$ meet at Γ_3 and after crossing it only the point E_1 survives becoming unstable. A separatrix asymptotic to E_1 keeps on surrounding E_5 and $\bar{E}_5$. This bifurcation is not the typical pitchfork bifurcation where two centres and a saddle merge in order to produce a centre, but in this case two saddles and a centre merge to end up with a saddle point.

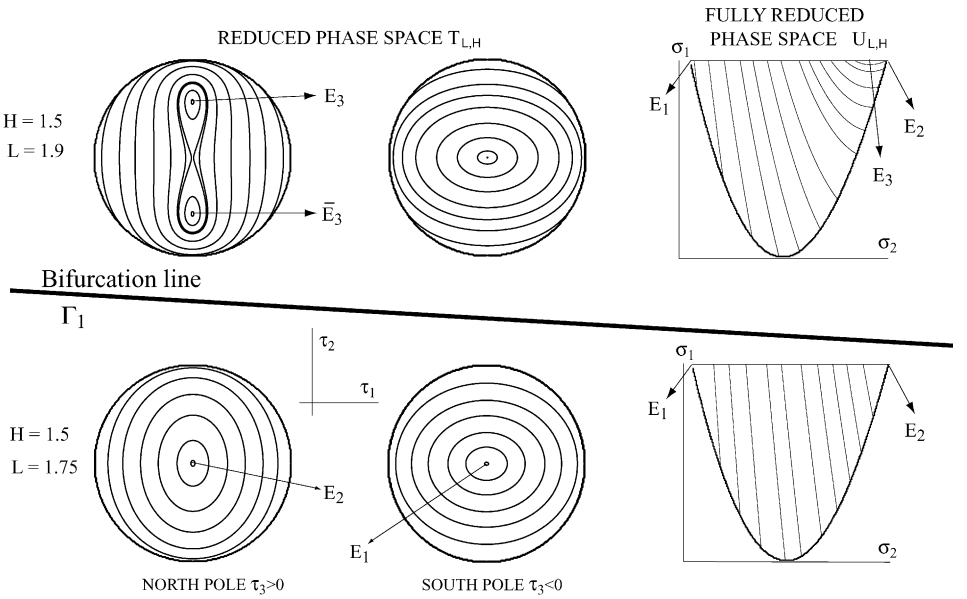

Fig. 5. Phase flow evolution of the system for $H = 1.5$ as L increases from 1.75 to 1.9. The first and second columns correspond to orthographic projections onto the plane (τ_1, τ_2) viewed from $\tau_3 > 0$ and from $\tau_3 < 0$, respectively, on the phase space $\mathcal{T}_{L,1.5}$. The third column corresponds to the same evolution in the fully-reduced phase space $\mathcal{U}_{L,1.5}$. Besides, $\delta = 0.01$ and $\beta = 0.4$.

After this second pitchfork bifurcation takes place and L increases, the two separatrices at E_1 and E_2 get close one each other, and when the curve Γ_6 is reached, both orbits collapse and a saddle-connection bifurcation takes place. After crossing Γ_6, the two separatrices interchange the centres they surround.

Finally, the evolution of the phase flow on the phase space $\mathcal{T}_{L,H}$ for fixed $L = 2.5$ and H increasing from 1.54 to 1.74 along a path crossing the bifurcation curves Γ_4 and Γ_2 is shown in Fig. 7. As H increases and the system approaches the curve Γ_4, the points E_2, E_5 and $\bar{E}_5$ get closer and when the line Γ_4 is crossed, another pitchfork

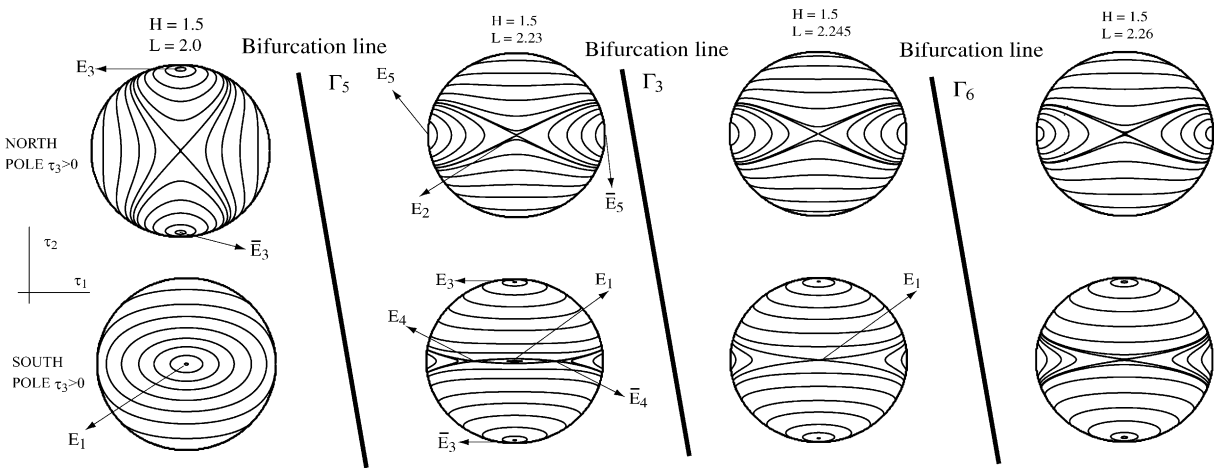

Fig. 6. Phase flow evolution of the system for $H = 1.5$ as L increases from 2 to 2.26. The first and second rows correspond to orthographic projections onto the plane (τ_1, τ_2) viewed from $\tau_3 > 0$ and from $\tau_3 < 0$, respectively, on the phase space $\mathcal{T}_{L,1.5}$. We have taken $\delta = 0.01$ and $\beta = 0.4$.

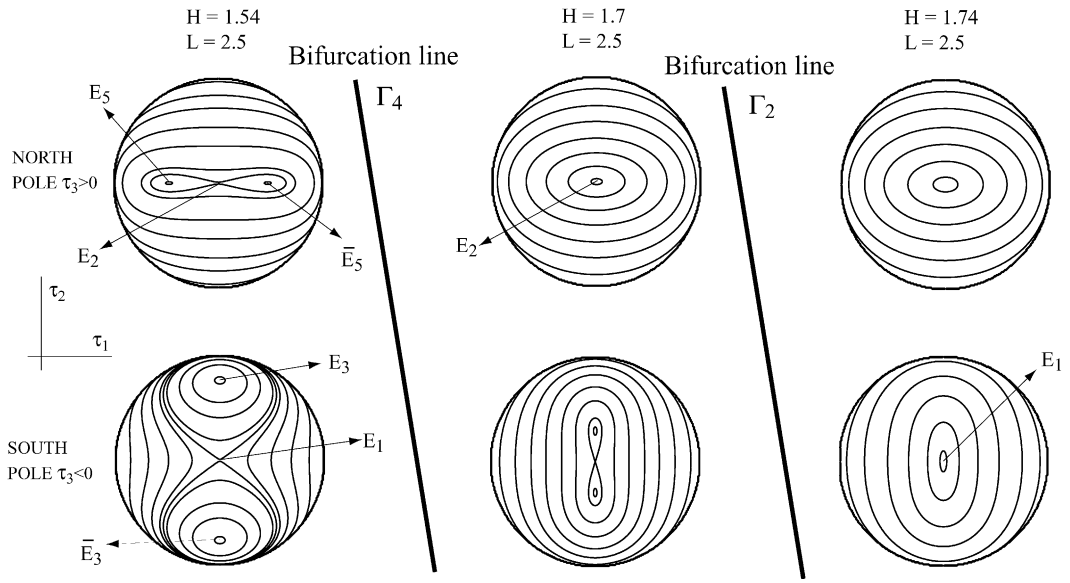

Fig. 7. Phase flow evolution of the system for $L = 2.5$ as H increases from 1.54 to 1.74. The first and second rows correspond to orthographic projections onto the plane (τ_1, τ_2) viewed from $\tau_3 > 0$ and from $\tau_3 < 0$, respectively, on the phase space $\mathcal{T}_{2.5,H}$. Besides, we take $\delta = 0.01$ and $\beta = 0.4$.

bifurcation takes place: the equilibria E_2, E_5 and $\bar{E}_5$ collapse, and after the bifurcation, only E_2 survives becoming stable.

The last bifurcation line, say Γ_2, is related to the appearance or disappearance of the equilibria E_1, E_3 and $\bar{E}_3$, and it corresponds to another pitchfork bifurcation. As H increases, the points E_1, E_3 and $\bar{E}_3$ approach one each other, and when Γ_2 is reached, all of the equilibria meet and only E_1 survives after the bifurcation.

7. Connection with the original system

7.1. Reconstruction of the flow defined by $\mathcal{H}$

Our next purpose is to approximate the invariant sets of the initial system from the critical points of the reduced one. We know [36] that for the case of toroidal symmetries—as the ones due to the appearance of the integrals L and H—we can generically continue a certain p-dimensional torus to a true $(p + n - s)$-dimensional torus of the initial Hamiltonian, where n designates the number of degrees of freedom of the original system and s the number of degrees of freedom of the reduced one. For our case, $p = 0$ (the only invariants determined in the fully-reduced Hamiltonian are equilibrium points), $n = 3$ and $s = 1$. Thus, (regular) critical points of $\bar{\bar{\mathcal{K}}}$ correspond to two-dimensional tori of $\mathcal{H}$. Once we have an equilibrium in the fully-reduced phase space, we can determine a family (parameterized by L and H) of invariant two-dimensional tori of the original Hamiltonian.

The procedure is as follows. Since $\bar{\bar{\mathcal{K}}}$ has been obtained after three reduction steps (the Keplerian reduction related to the first-order normalisation followed by the exact axial-symmetry reduction and the reduction by the discrete symmetries), in order to pass to the original Hamiltonian we should attach either a family of two-dimensional invariant tori (with parameters L and H) to any point of $\mathcal{T}_{L,H}$ if $|H| > 0$ or either a family of periodic orbits (parameterized by L) to the singular points $(\pm L, 0, 0)$ of $\mathcal{T}_{L,0}$. However, we notice that the points $(\pm L, 0, 0)$ must be discarded as all our Hamiltonians (perturbations of the two-body system) are singular for rectilinear orbits.

We also need to discard those critical points whose linearisation has null eigenvalues. If $|H| < G < L$, the two-dimensional tori are defined by the angles ℓ and h. In case of equatorial ($G = |H|$) or circular motions ($G = L$) it is still possible to define other action and angle variables and perform the reconstruction of the invariant tori similarly, as we will see later on when trying to get closed orbits.

What we obtain about the original system are families of two-dimensional invariant tori depending on the parameters L and H but also on the external parameters β and δ. An equilibrium on the fully-reduced phase spaces, whose linearisation has no null eigenvalue, must be in correspondence with one, two or four families of two-dimensional invariant tori in $\mathbf{R}^6$, depending on where these points are placed in the fully-reduced phase space. Moreover, an equilibrium in the fully-reduced phase space and its corresponding invariant torus share the same type of stability (nonlinear in the hyperbolic case).

For those equilibria of $\mathcal{U}_{L,H}$ or of $\mathcal{U}_{L,0}$ where the linearisation yields null eigenvalues, a specific analysis should be performed. This situation occurs here only for the saddle-centre and pitchfork bifurcations. For a detailed analysis and reconstruction of the flow for the former we refer to [7] whereas the latter have been studied in [17]. In both cases, the degenerate points are of parabolic type and therefore unstable. So, the corresponding two-dimensional tori are also parabolic as the fully-reduced system is structurally stable.

We can even compute the explicit formulae of the approximations of the two-dimensional invariant tori using the direct change of the Delaunay normalisation, i.e. the transformation α, inserting thereafter the coordinates of E_i in this change. However, on the one hand, we have detected families of quasiperiodic orbits of equatorial and circular type. On the other hand, Delaunay coordinates are not defined for these orbits. Thus, we resort to a different set of action and angle variables well defined for small inclinations and all eccentricities $e \in [0, 1)$: the set of canonical Poincaré elements [25]:

$$\begin{aligned} &q_1 = \ell + g + h, \qquad q_2 = -\sqrt{2(L-G)}\,\sin(g+h), \qquad q_3 = \ell + g, \\ &p_1 = L - G + H, \qquad p_2 = \sqrt{2(L-G)}\,\cos(g+h), \qquad p_3 = G - H. \end{aligned} \tag{35}$$

Now we construct the transformation α referred to the variables (35). This is achieved using the change α and taking into account the partial derivatives among the Poincaré and Delaunay elements. Besides, we need to express the coordinates of the particular point E_i in terms of (35). Hence, an invariant torus related to a specific equilibrium point E_i is defined through the angles q_1 and q_3. Note that G and g are functions of the parameters L and H and consequently we have obtained a (two-parameter) family of two-dimensional tori for a given critical point E_i. In this case, a first-order normalisation has been enough to study the qualitative dynamics of the original problem. Nevertheless, provided that the global error after truncation be maintained small enough, the higher the order we reach with the Lie transformation, the more accurate the invariant tori of $\mathcal{H}$ are.

The approximated tori of the system defined by $\mathcal{H}$ are indeed approximations of true invariant tori. Their existence can be guaranteed because the two continuous symmetries are action variables conjugated to angular coordinates. Thus, we can define a suitable Poincaré mapping and apply the Implicit Function Theorem, details appear in [36]. Generically the true tori can be refined using either analytical or numerical continuation techniques. Next, bifurcations of relative equilibria are translated into bifurcations of families of two-dimensional invariant tori or quasiperiodic orbits. The persistence of these bifurcations is guaranteed by the estimate of the next subsections.

We do not give details about the reconstruction of the full system using KAM theory, as the analysis is analogous to the ones performed in [7,17]. Instead, we illustrate the connection to the original system by using estimates of the error for the transformations Φ or α, as well as some surfaces of section.

7.2. Error estimation

We estimate the error to show the range of validity of the results obtained and consequently the reliability of the conclusions on the original system. Estimates on the time validity of the Delaunay normalisation (at first order or

at higher orders) can be directly derived from the generating function and the inverse change obtained in Section 3 through Eq. (9).

If we denote $\mathbf{z} = (\ell, g, h, L, G, H)$ and $\mathbf{y} = (\ell', g', h', L', G', H')$, we know that $\Phi(\mathbf{y}) = \mathbf{z} + \mathcal{O}(\delta^2)$ and $\alpha(\mathbf{z}) = \mathbf{y} + \mathcal{O}(\delta^2)$. We can compose $\mathcal{H}$ with Φ or $\mathcal{K}$ with α getting:

$$\mathcal{H}(\mathbf{z}) - \mathcal{K}(\mathbf{y}) = \mathcal{H}(\alpha(\mathbf{y})) - \mathcal{K}(\mathbf{y}) = \mathcal{O}(\delta^2),$$

$$\mathcal{K}(\mathbf{y}) - \mathcal{H}(\mathbf{z}) = \mathcal{K}(\Phi(\mathbf{z})) - \mathcal{H}(\mathbf{z}) = \mathcal{O}(\delta^2).$$

The error term $\mathcal{O}(\delta^2)$ is a function of $\mathbf{y}$ or of $\mathbf{z}$ and the parameters β and δ. Moreover, δ acts as a small parameter.

We prefer to compose $\mathcal{K}$ with α and work with the initial Delaunay coordinates $\mathbf{z}$, since we can make comparisons with the original Hamiltonian. Now, the error $\mathcal{O}(\delta^2)$ can be written as:

$$\mathcal{K}(\Phi(\mathbf{z})) - \mathcal{H}(\mathbf{z}) = \epsilon(\mathbf{z}),$$

where ϵ plays the role of the global error produced by truncating the computation at degree one. The maximum of $|\epsilon(\mathbf{z})|$ evaluated for different values of $\mathbf{z}$ will give us the size of the error. This function depends on five coordinates—h is not present in the formulae—plus the constant β. Next we need to evaluate $\epsilon(\mathbf{z})$ with the angles ℓ and g allowed to vary in $[0, 2\pi)$ whereas L, G and H satisfy $0 \leq |H| \leq G \leq L$. Besides, we take $\beta \in [0, 0.5]$ and build a grid of 1000 points. We have checked that $\max|\epsilon(\mathbf{z})| < 2\delta^2$ and consequently the theory can be considered of order one.

We can conclude that the composition given in the above paragraph is true on a time-scale of $1/\delta$, that is, the transformation of $\mathcal{H}$ into $\mathcal{K}$ and the changes of coordinates are valid for $t \in [0, C/\delta]$ for some constant $C > 0$, see reference [27] for details and workout examples. However, in practice it is not always easy to determine the majorant C and this is usually done in every particular situation. Other upper bounds of the time validity could be obtained using Nehorošev theory, though it is outside the scope of the present paper.

7.3. Poincaré surfaces of section

The analytical results obtained in the previous sections may be validated by means of Poincaré surfaces of section. Even more, the results of this section are in agreement with the estimation of the error studied in Section 7.2.

To begin with, we recall that periodic orbits are reflected as fixed points on the Poincaré surfaces of section. Thus, every fixed point on the surface of section can be associated with an equilibrium in the fully-reduced phase space.

We define the surface of section as $z = 0$ and $P_z \geq 0$ from Hamiltonian (7). This surface appears as a closed region in the plane (ρ, P_ρ) bounded by:

$$P_\rho = \pm\sqrt{2E - \frac{\delta^2}{\rho^4} + \frac{2\delta H}{\rho^3} - \frac{H^2}{\rho^2} + \frac{2}{\rho} - \frac{2\beta\delta}{\rho}}, \tag{36}$$

for a fixed value of the energy $E = \mathcal{H} < 0$. Note that the equatorial oscillation on the ρ-axis, which always exists, is tangent to the flow in this representation, and corresponds to the exterior limit of the Poincaré section. This periodic orbit corresponds to the equilibrium point E_1 in the fully-reduced phase space. Besides, since this orbit does not appear as a single fixed point, its stability cannot be determined directly by looking at the orbits around it. However, the stability character can be inferred from the Index Theorem [26].

We set $\delta = 0.01$ and $\beta = 0.4$, whereas the energy $E \approx -1/(2L^2)$ and the z-component H of the angular momentum are conveniently varied in order to sweep out the different regions where changes in the dynamics are expected.

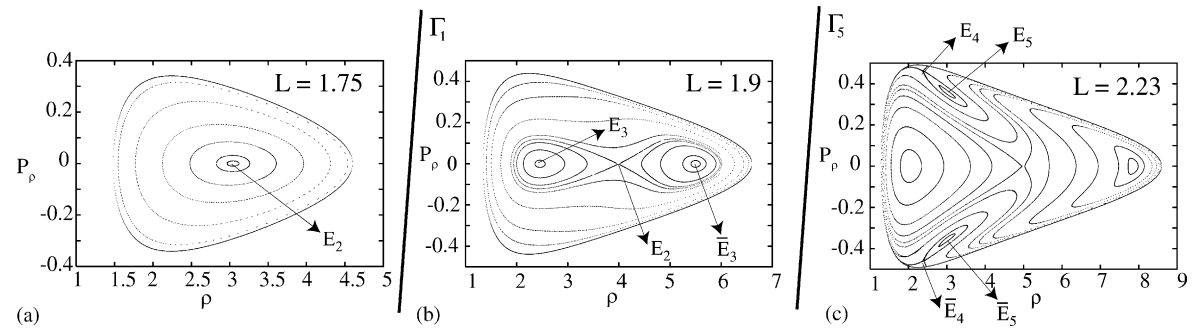

Fig. 8. Evolution of the surfaces of section $z = 0$ and $P_z \geq 0$ for $\delta = 0.01$, $\beta = 0.4$, $H = 1.5$ and (a) $L = 1.75$, (b) $L = 1.9$ and (c) $L = 2.23$.

The first bifurcation we are looking for is a pitchfork one and it occurs when Γ_1 is crossed. This bifurcation is depicted in Fig. 8. For $H = 1.5$ and $L = 1.75$, the stable fixed point in Fig. 8a is an almost circular orbit which corresponds to the equilibrium E_2 in the fully-reduced phase space. For $L = 1.9$ (see Fig. 8b), the pitchfork bifurcation takes place: the fixed point E_2 becomes unstable and the separatrix passing through it surrounds two new stable fixed points, which correspond to the equilibria E_3 and $\bar{E}_3$ in the fully-reduced phase space. Besides, E_1 is stable for both $L = 1.75$ and $L = 1.9$.

When the bifurcation line Γ_5 is crossed, a double saddle-centre bifurcation is expected. This bifurcation can be seen in Fig. 8c for $L = 2.23$. In the upper and lower corners of the section, there appear four new fixed points which correspond to the two stable equilibria E_5 and $\bar{E}_5$ and to the two unstable equilibria E_4 and $\bar{E}_4$ in the twice-reduced phase space.

A clearer vision of this bifurcation can be obtained by changing the definition of the surface of section to a new one where the equatorial periodic orbit E_1 is inside the surface of section. This can be achieved by defining the surface as the section $\rho = \rho_o$ and $P_\rho \geq 0$. This time the boundary of the surfaces of section is obtained by expressing P_z in terms of z in Eq. (7) after replacing $\rho = \rho_o$ and $P_\rho = 0$. We note that with this unusual surface of section, we cannot guarantee that it will be crossed by most of the orbits [14]. In Fig. 9, a sequence of three surfaces of section defined by $\rho = 4$ and $P_\rho \geq 0$ is shown. The double saddle-centre bifurcation may be observed comparing the surfaces of section given in Fig. 9a and b.

The next bifurcation is a pitchfork one and it takes place when the line Γ_3 is crossed (compare Fig. 9b and c).

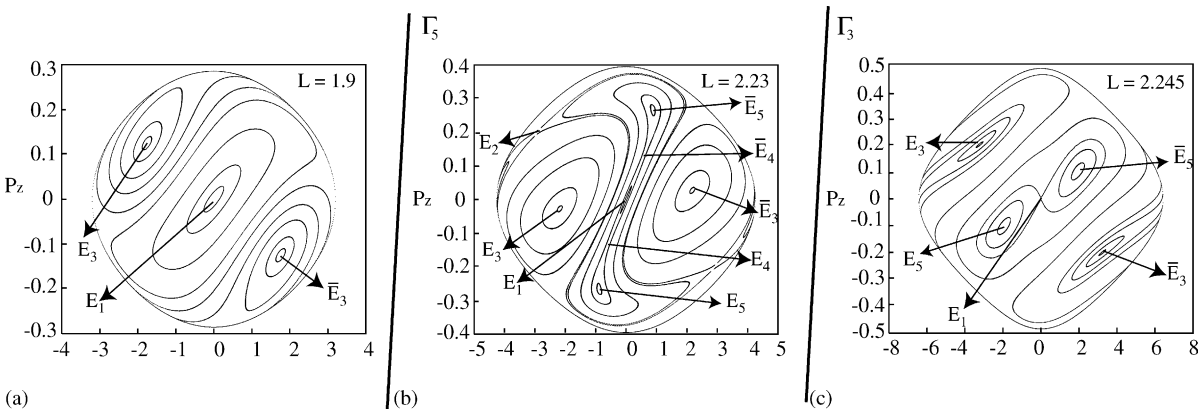

Fig. 9. Evolution of the surfaces of section $\rho = 4$ and $P_\rho \geq 0$ for $\delta = 0.01$, $\beta = 0.4$, $H = 1.5$ and (a) $L = 1.9$, (b) $L = 2.23$, (c) $L = 2.245$.

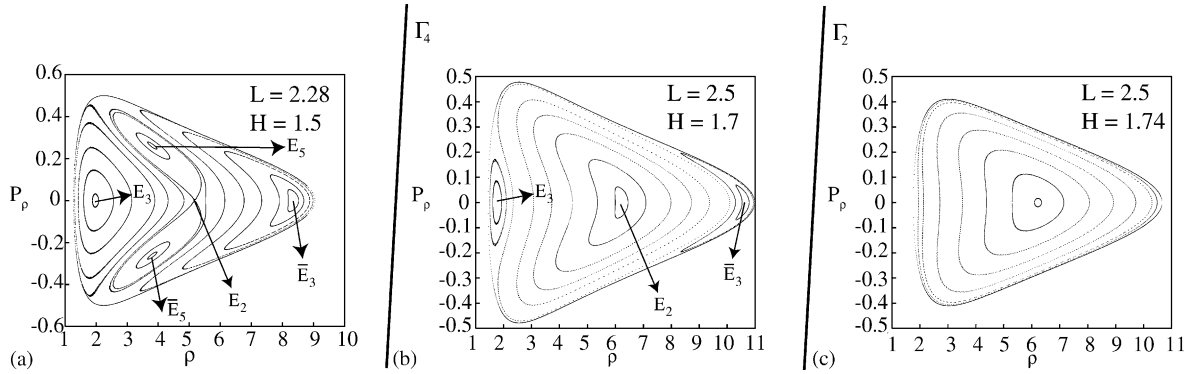

Fig. 10. Evolution of the surfaces of section $z = 0$ and $P_z \geq 0$ for $\delta = 0.01$, $\beta = 0.4$ and (a) $L = 2.28$ and $H = 1.5$, (b) $L = 2.5$ and $H = 1.7$, (c) $L = 2.5$ and $H = 1.74$.

The saddle-connection bifurcation is observed when Fig. 10a is compared to Fig. 8b and c. Note that while in Fig. 8b and c the separatrix passing through E_2 surrounds the fixed points E_3 and $\bar{E}_3$, in Fig. 10a this separatrix surrounds E_5 and $\bar{E}_5$. Finally, in Fig. 10b and c, the last two pitchfork bifurcations—which take place when the lines Γ_4 and Γ_2 are crossed—are reported.

It is worth mentioning that the values of the parameters for which the bifurcations are observed in the surfaces of section are in very good agreement with the values of the parameters for the bifurcation lines of Section 5.

7.4. Symmetric periodic orbits

Even though it is possible to determine periodic orbits from surfaces of section, now we see how some quasiperiodic orbits of the original system turn into periodic orbits under certain assumptions. Here, we determine families of symmetric and doubly-symmetric periodic orbits. These doubly-symmetric orbits have been analysed in the context of the restricted three-body problem by various authors, and we cite the recent reference [25]. Here, we follow the steps of [37] adapted for our requirements.

As discussed already in Section 4, Hamilton function (5) is invariant under the reflections given in (16). We choose $\mathcal{R}_1$ and $\mathcal{R}_2$ as fundamental symmetries since $\mathcal{R}_3$ can be generated combining $\mathcal{R}_1$ and $\mathcal{R}_2$. In Cartesian coordinates, $\mathcal{R}_1$ and $\mathcal{R}_2$, respectively, fix the hyperplanes $\mathcal{L}_1$ and $\mathcal{L}_2$ defined by:

$$\mathcal{L}_1 = \{(x, 0, 0, 0, P_y, P_z) \mid x, P_y, P_z \in \mathbf{R}\},$$
$$\mathcal{L}_2 = \{(x, 0, z, 0, P_y, 0) \mid x, z, P_y \in \mathbf{R}\}.$$

Now we take advantage of the discrete symmetries with the aim of closing some of the quasiperiodic solutions predicted in Section 7.1. Using Poincaré coordinates (35) the fixed hyperplanes read as:

$$\mathcal{L}_1 = \{(q_1, 0, q_3, p_1, p_2, p_3) \quad \text{with} \quad q_1 \equiv q_3 \equiv 0 \bmod \pi\},$$
$$\mathcal{L}_2 = \{(q_1, 0, q_3, p_1, p_2, p_3) \quad \text{with} \quad q_1 \equiv 0 \bmod \pi, q_3 \equiv \tfrac{1}{2}\pi \bmod \pi\}.$$

To get an approximation of a closed orbit of Hamiltonian $\mathcal{H}$ we look for a linear relation between the angles q_1 and q_3. Indeed, we use the hyperplanes $\mathcal{L}_1$ and $\mathcal{L}_2$ to pick some initial conditions, ensuring that a certain trajectory starting at $\mathcal{L}_1$ will get closed at the same point of $\mathcal{L}_1$ and the same applies for initial conditions in $\mathcal{L}_2$. Note that we have a certain freedom since we have families of quasiperiodic trajectories parameterized by L and H. Thus, we

set $q_3 = q_3^0 + s(q_1 - q_1^0)$ for some initial conditions q_1^0 and q_3^0 that we shall fix later on. The determination of the slope s is made through the quotient

$$s = \frac{\mathrm{d}q_3}{\mathrm{d}q_1} = \frac{\mathrm{d}q_3/\mathrm{d}t}{\mathrm{d}q_1/\mathrm{d}t}.$$

In order to calculate it we go back to Hamiltonian (10). As we know that $\mathrm{d}\ell/\mathrm{d}t = \partial\mathcal{K}/\partial L$, $\mathrm{d}g/\mathrm{d}t = \partial\mathcal{K}/\partial G$ and $\mathrm{d}h/\mathrm{d}t = \partial\mathcal{K}/\partial H$, we get: $\mathrm{d}q_3/\mathrm{d}t = \partial\mathcal{K}/\partial L + \partial\mathcal{K}/\partial G$ and $\mathrm{d}q_1/\mathrm{d}t = \partial\mathcal{K}/\partial L + \partial\mathcal{K}/\partial G + \partial\mathcal{K}/\partial H$. Now, $\cos g$, $\sin g$ and G are written in terms of the σ's using Eq. (20) and finally the coordinates of the equilibria E_i, say, $(\sigma_{1_i}^0, \sigma_{2_i}^0)$, are substituted into the resulting expressions. Thus, we compute the possible slopes s for all critical points E_i and conclude that s is a function of the four parameters δ, β, L and H.

Three possibilities are in order: periodic orbits intersecting $\mathcal{L}_1$, or $\mathcal{L}_2$, or both hyperplanes. They are symmetric in the first two cases and doubly-symmetric in the last one. For instance, if one is interested in calculating the closed orbits intersecting $\mathcal{L}_1$, we select initial conditions $q_1^0 \equiv q_3^0 \equiv 0 \bmod \pi$ and $q_2^0 = 0$.

As an illustration, we detail how to obtain periodic orbits out of the quasiperiodic orbits related to the equilibria E_1 and E_2. In both cases, using (20) we have that $\sin g = 0$, then we take $h_0 = 0$ and $q_2^0 = 0$. Hence, choosing $\ell_0 = 0$ we get $q_1^0 = q_3^0 = 0$ and the relations among the angles yield:

$$\begin{aligned} q_3 &= \frac{ep_n}{ep_d} q_1 \quad \text{for} \quad G = H, \\ q_3 &= \frac{er_n}{er_d} q_1 \quad \text{for} \quad G = -H, \\ q_3 &= \frac{c_n}{c_d} q_1 \quad \text{for} \quad G = L, \end{aligned} \tag{37}$$

where

$$\begin{aligned} ep_n &= -8L^3H^6(L+H) + \delta^2(L+H)(35L^3 - 7LH^2 + 18L^2H - 10H^3) \\ &\quad + 8\delta L^2H^3[-3H^2 + 2LH(-3 + \beta H^3) + L^2(-3 + 4\beta H^3)], \\ ep_d &= 2(L+H)[-4L^3H^6 + \delta^2(15L^3 - 5H^3 - 3LH^2 + 9L^2H) \\ &\quad + 4\delta L^2H^3(-2L - 3H + 2\beta LH^3)], \end{aligned}$$

and similar expressions hold for er_n, er_d, c_n and c_d.

Next we go back to the (approximate) expressions obtained in Section 7.1 for the families of two-dimensional invariant tori associated with equatorial and circular motions of the original Hamiltonian $\mathcal{H}$. Then we express these tori in Poincaré variables using (35). Thereafter, we make that the angular variables of the tori q_3 and q_1 satisfy one of the conditions given through (37), obtaining (approximate) families of periodic orbits, parameterized by L and H which are either nearly equatorial—both prograde and retrograde—or nearly circular.

Other approximations of periodic orbits for other critical points of $\bar{\bar{\mathcal{K}}}$ can be determined similarly. However, note that we do not know the explicit form of the critical points $(\sigma_{1i}^0, \sigma_{2i}^0)$ excepting for equatorial and circular orbits. Anyway one can give particular values for L and H in a specific region of the plane of parameters and proceed as in the preceding paragraphs. We also encounter periodic orbits from the quasiperiodic orbits related to E_i, but using the symmetry $\mathcal{R}_2$. It is achieved by taking the corresponding slopes s and initial conditions q_i^0 and p_i^0 adequately. This collection of closed trajectories are again generically parameterized by L and H.

Next we show how to get doubly-symmetric closed orbits. In order to do so we need that the trajectory touches the two fixed hyperplanes. We start by taking initial conditions in $\mathcal{L}_1$, forcing the solution to pass through $\mathcal{L}_2$ and ending in $\mathcal{L}_1$ in the same initial conditions. So, we make $q_2^0 = 0$, $q_1^0 = j\pi$ and $q_3^0 = k\pi$ with $j, k \in \mathbf{Z}$. Now we impose that

our closed orbit reaches $\mathcal{L}_2$, i.e. we make $q_2^1 = 0$, $q_1^1 = m\pi$ and $q_3^1 = \pi/2 + n\pi$, where $m, n \in \mathbf{Z}$. Observe now that the equation $q_3 = q_3^0 + s(q_1 - q_1^0)$ has to be satisfied by the pair (q_3^1, q_1^1). Thence, we arrive at the relation:

$$k + s(m - j) - \tfrac{1}{2} - n = 0, \tag{38}$$

where the slope s depends on the equilibrium point we choose. For instance, we start by giving the following values for the external parameters: $\delta = 0.01$ and $\beta = 0.4$. Now we select the values of the integrals H and L doing $H = 1$ and $L = 3$. With these choices we compute the slope s through the quotient c_n/c_d, obtaining a rational value for s which may be approximated by $0.999\ldots$. Next, we put $m = n = 0$ and try to adjust the integers j and k so that Eq. (38) can be satisfied. After setting $j = 65401001$, we get $k = 65337820$. Thus, we have obtained a closed orbit of circular type, which according to condition (33) is unstable. It is even unstable taking the whole $\overline{\overline{\mathcal{K}}}$.

Other stable and unstable periodic trajectories of $\mathcal{H}$ can be obtained in a similar way, taking appropriate initial conditions in either $\mathcal{L}_1$ or $\mathcal{L}_2$ and passing either through $\mathcal{L}_2$ or through $\mathcal{L}_1$, respectively.

Proceeding as in the previous paragraphs, we have obtained single-symmetric and doubly-symmetric periodic orbits ranking from circular ($G = L$) to almost rectilinear ($G \approx 0$) and having inclinations varying from 0 to nearly π. Besides, the stability of such orbits depends on the values of L and H, according to the region of the plane of parameters in correspondence with the fixed values of L and H. We stress the importance of obtaining a closed-form expression of $\mathcal{W}_1$, as we have got formulae for all type of elliptic motions.

The approximate periodic orbits we have obtained can be refined either analytically or numerically. Numerical strategies to continue periodic orbits of Hamiltonian problems can be looked up in [28], whereas analytical techniques are based on the calculation of higher-order terms of Hamiltonian $\mathcal{K}$—or Hamiltonian $\overline{\overline{\mathcal{K}}}$—using Lie transformations, combined with the analytical approximation of the critical points of $\overline{\overline{\mathcal{K}}}$ which are needed to get a good approximation of a certain trajectory.

8. Conclusions

We have studied the dynamics of a charged particle that orbits a rotating magnetic planet. We have focused on the Keplerian regime, i.e. on the case where the main force acting over the particle is the gravitational field created by the planet. The main features of our work can be summarized as follows:

(i) We have made a rigorous analysis of the *GS* problem, establishing two-dimensional invariant tori and quasiperiodic orbits together with their stability. The occurrence and type of stability of the invariant tori and quasiperiodic orbits depend on four parameters, two of them being of external nature: β and δ, and the other two of internal character: the exact integral of the problem H and the approximate integral L. Besides, we have determined analytically the bifurcation lines, i.e. the relations among the four parameters so that a change in the number of invariant tori and stability happens. The *GS* Hamiltonian presents a very rich dynamics depending on its parameters. Indeed, we have found a saddle-centre, five pitchfork as well as a saddle-connection bifurcation. Besides, we have tested their existence using Poincaré surfaces of section.

(ii) The analysis has been possible through a simplification of the original Hamiltonian. First of all, a Delaunay normalisation has been utilized to average the Hamilton function with respect to the mean anomaly. A method for controlling the error related to the truncation of the averaged Hamiltonian has been used. Then, we have applied reduction theory to express the averaged Hamiltonian, truncated at first order, in terms of functions invariant with respect to the two continuous symmetries of the resulting problem: the axial one and the symmetry induced by averaging. Next, we have taken advantage of the finite symmetries of the problem to construct the fully-reduced Hamiltonian in its corresponding two-dimensional phase space.

(iii) The fully-reduced Hamiltonian defines a system of one degree of freedom and is therefore easier to be studied than the original one. We have extracted the qualitative information about its critical points. This is translated

to the original Hamiltonian using reconstruction of the flow techniques. Besides, we have plotted the flow of the twice-reduced Hamiltonian and the one corresponding to the fully-reduced system. By doing so we have verified the occurrence of all bifurcations found analytically.

(iv) Some true symmetric periodic orbits of the original Hamiltonian have been approximated to first order using the finite symmetries of the problem. These periodic orbits can be either continued numerically using standard methods or analytically approximated pushing the normalisation to higher orders. We plan to tackle this issue in future.

(v) We have enlarged the study done in [24,23,13], finding a new collection of periodic trajectories crossing the equatorial plane of the planet's orbit.

The methodology used in this paper can be applied to other problems formulated as perturbations of the two-body problem, enjoying an axial symmetry or not, but enjoying a set of discrete symmetries like those of (16). We cite some problems related to the restricted three-body Hamiltonian (see [29,37]), an artificial satellite orbiting a planet where the perturbation caused by the gravity field of the planet is taken into account (see also [9,6]), the hydrogen atom under the influence of an electric and a magnetic crossed fields (see, for instance, [8,15]) or some problems of physical chemistry, modelled by means of the so-called generalised van der Waals potential [16].

Acknowledgments

This work has been partially supported by Project # BFM2002-03157 of Ministerio de Ciencia y Tecnología (Spain), Project # ACPI2002/04 of Departamento de Educación y Cultura, Gobierno de La Rioja (Spain), Project # API02/20 of Universidad de La Rioja (Spain) and Project Resolución 92/2002 of Departamento de Educación y Cultura, Gobierno de Navarra (Spain).

References

[1] J.M. Arms, R.H. Cushman, M.J. Gotay, A universal reduction procedure for Hamiltonian group actions, in: T. Ratiu (Ed.), The Geometry of Hamiltonian Systems. M.R.S.I. Workshop Proceedings, Springer-Verlag, Berlin/New York, 1991, pp. 33–51.
[2] M. Braun, Particle motions in a magnetic field, J. Differential Equations 8 (1970) 294–332.
[3] M. Braun, Structural stability and the Størmer problem, Indiana Univ. Math. J. 20 (1970) 469–497.
[4] D. Brouwer, G.M. Clemence, Methods of Celestial Mechanics, Academic Press, New York/London, 1961.
[5] D. Cox, J. Little, D. O'Shea, Ideals, Varieties and Algorithms: An Introduction to Computational Algebraic Geometry and Commutative Algebra, Springer-Verlag, Berlin/New York, 1992.
[6] R.H. Cushman, Reduction, Brouwer's Hamiltonian, and the critical inclination, Celestial Mech. 31 (1983) 401–429.
[7] R.H. Cushman, S. Ferrer, H. Hanßmann, Singular reduction of axially symmetric perturbations of the isotropic harmonic oscillator, Nonlinearity 12 (1999) 389–410.
[8] R.H. Cushman, D.A. Sadovskií, Monodromy in the hydrogen atom in crossed fields, Physica D 142 (2000) 166–196.
[9] A. Deprit, The elimination of the parallax in satellite theory, Celestial Mech. 24 (1981) 111–153.
[10] A. Deprit, Delaunay normalisations, Celestial Mech. 26 (1982) 9–21.
[11] A. Dragt, Trapped orbits in a magnetic dipole field, Rev. Geophys. 3 (1965) 255–298.
[12] A. Dragt, J. Finn, Insolubility of trapped particle motion in a magnetic dipole field, J. Geophys. Res. 81 (1976) 2327–2340.
[13] H.R. Dullin, M. Horányi, J.E. Howard, Generalizations of the Størmer problem for dust grain orbits, Physica D 171 (2002) 178–195.
[14] H.R. Dullin, A. Wittek, Complete Poincaré sections and tangent sets, J. Phys. A 28 (1995) 7157–7180.
[15] K. Efstathiou, R.H. Cushman, D.A. Sadovskií, Hamiltonian Hopf bifurcation of the hydrogen atom in crossed fields, Physica D 194 (2004) 250–274.
[16] A. Elipe, S. Ferrer, Reductions, relative equilibria and bifurcations in the generalized van der Waals potential: relation to the integrable cases, Phys. Rev. Lett. 72 (1994) 985–988.
[17] S. Ferrer, H. Hanßmann, J. Palacián, P. Yanguas, On perturbed oscillators in 1-1-1 resonance: the case of axially symmetric cubic potentials, J. Geom. Phys. 40 (2002) 320–369.

[18] A.M. Fridman, N.N. Gor'kavyi, Physics of Planetary Rings: Celestial Mechanics of Continuous Media, Springer-Verlag, Berlin/New York, 1999.
[19] R. Grard, A. Balogh (Eds.), Returns to Mercury: Science and Mission Objectives, Planet. Space Sci. 49 (2001) 1395–1692 (Special issue).
[20] D.P. Hamilton, Motion of dust in a pleanetary magnetosphere: orbit-averaged equations for oblateness, electromagnetic and radiation forces with application to Saturn's E ring, Icarus 101 (1993) 244–264 (Erratum, Icarus 103 (1993) 161).
[21] L. Healy, E. Deprit, Paint by number: uncovering phase flows of an integrable dynamical system, Comput. Phys. 5 (1991) 491–496.
[22] M. Horányi, Charged dust dynamics in the solar system, Annu. Rev. Astronom. Astrophys. 34 (1996) 383–418.
[23] J.E. Howard, H.R. Dullin, M. Horányi, Stability of halo orbits, Phys. Rev. Lett. 84 (2000) 3244–3247.
[24] J.E. Howard, M. Horányi, G.E. Stewart, Global dynamics of charged dust particles in planetary magnetospheres, Phys. Rev. Lett. 83 (1999) 3993–3996.
[25] R.C. Howison, K.R. Meyer, Doubly-symmetric periodic solutions of the spatial restricted three-body problem, J. Differential Equations 163 (2000) 174–197.
[26] M. Iñarrea, J.P. Salas, V. Lanchares, Hydrogen atom in the presence of uniform magnetic and quadrupolar electric fields: Integrability, bifurcations, and chaotic behavior, Phys. Rev. E 66 (12) (2002) 056614.
[27] N. Krylov, N. Bogoliubov, Introduction to Nonlinear Mechanics, Academic Press, New York, 1947.
[28] M. Lara, On numerical continuation of families of periodic orbits in a parametric potential, Mech. Res. Commun. 23 (1996) 291–298.
[29] M.L. Lidov, S.L. Ziglin, Non-restricted double-averaged three body problem in Hill's case, Celestial Mech. 13 (1976) 471–489.
[30] K.R. Meyer, Symmetries and integrals in mechanics, in: M.M. Peixoto (Ed.), Dynamical Systems, Academic Press, New York/London, 1973, pp. 259–272.
[31] L. Milnor, Morse Theory, Annals of Mathematics Studies, vol. 51, Princeton University Press, Princeton, NJ, 1963.
[32] J. Moser, Regularization of Kepler's problem and the averaging method on a manifold, Commun. Pure Appl. Math. 23 (1970) 609–636.
[33] C.D. Murray, S.F. Dermott, Solar System Dynamics, Cambridge University Press, Cambridge, 1999.
[34] C. Osácar, J. Palacián, Decomposition of functions for elliptic orbits, Celestial Mech. Dyn. Astronom. 60 (1994) 207–223.
[35] J. Palacián, Normal forms for perturbed Keplerian systems, J. Differential Equations 180 (2002) 471–519.
[36] J. Palacián, Invariant manifolds of an autonomous ordinary differential equation from its generalised normal forms, Chaos 13 (2003) 1188–1204.
[37] J. Palacián, P. Yanguas, Invariant manifolds of spatial restricted three-body problems: the lunar case, in: J. Delgado, E.A. Lacomba, J. Llibre, E. Pérez-Chavela (Eds.), New Advances in Celestial Mechanics and Hamiltonian Systems, Kluwer Academic/Plenum Publishers, Dordrecht, 2004, pp. 199–221.
[38] C. Størmer, Sur les trajectories des corpuscules electrices, Arch. Sci. Phys. Nat. 24 (1907) 5–18, 113–158, 221–247.
[39] C. Størmer, The Polar Aurora, Clarendon Press, Oxford, 1955.
[40] TRANSFORM, Fortner Research LLC, Sterling, VA 20164, 1996.
[41] E.T. Whittaker, A Treatise on the Analytical Dynamics of Particles and Rigid Bodies, Cambridge University Press, Cambridge, 1927.